College of Engineering and Applied Science 428 UCB Boulder, Colorado 80309-0428

<u>CIEST@colorado.edu</u> website:<u>www.colorado.edu/center/ciest</u>

t: 303.492.8221

Center for Infrastructure, Energy, & Space Testing

Experimental Assessment of PVC Pipe Joint with RieberLok Gasket under Axial Loading

Testing Report

Submitted to:

Timothy C. Lango Northern Pipe Products

Prepared by:

Ceylan, M.

Ihnotic, C.

Wham, B.P.



Center for Infrastructure, Energy, and Space Testing Civil, Environmental, and Architectural Engineering University of Colorado Boulder Boulder, CO 80309

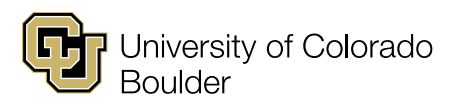
September 2024



College of Engineering and Applied Science 428 UCB Boulder, Colorado 80309-0428 t: 303.492.8221 CIEST@colorado.edu website:www.colorado.edu/center/ciest

Table of Contents

Table of Contents	2
List of Figures	4
List of Tables	7
1. Introduction	8
1.1 Test Specimens	8
1.2 Test Overview	9
2. Axial Testing	10
2.1 Axial Test Setup	10
2.1.1 Specimen Installation Procedur	e12
2.1.2 Instrumentation	14
2.2 Axial Test Procedure	14
2.2.1 Pretest	14
2.2.2 Tension Test Sequence	
2.2.3 Cyclic Test Sequence	
2.2.4 Stop or Pause Criteria	16
3. Axial Tension Test Results	17
3.1 Tension Test (PT44)	17
3.2 Tension Test (PT45)	20
3.3 Tension Test (PT46)	22
3.4 Tension Test (PT50)	25
3.5 Tension Test (PT51)	27
3.6 Tension Test (PT52)	29
3.7 Tension Test Overview	32
4. Axial Cyclic Test Results	35
4.1 Cyclic Test (PS47)	35
4.2 Cyclic Test (PS48)	37
	40
4.4 Cyclic Test (PS53)	42
4.5 Cyclic Test (PS54)	45
4.6 Cyclic Test (PS55)	49
4.7 Cyclic Test Overview	52
5. Conclusions	54



College of Engineering and Applied Science 428 UCB Boulder, Colorado 80309-0428

t: 303.492.8221 CIEST@colorado.edu

website: www.colorado.edu/center/ciest

Center for Infrastructure, Energy, & Space Testing

Acknowledgments	55
-	
References	55



College of Engineering and Applied Science 428 UCB Boulder, Colorado 80309-0428

t: 303.492.8221 CIEST@colorado.edu website:www.colorado.edu/center/ciest

List of Figures

Figure 1.1. Example of a typical bell/spigot joint for a) Northern Pipe and b) VinylTech	9
Figure 2.1. Axial test setup in the loading frame 1	10
Figure 2.2. Axial test setup in the loading frame 2	11
Figure 2.3. Dimensioned drawing of axial test setup for frame 1	11
Figure 2.4. Dimensioned drawing of axial test setup for frame 2	11
Figure 2.5. Marked measurements on spigot	12
Figure 2.6. Installation of RieberLok gasket	12
Figure 2.7. Bell and spigot before joint insertion	12
Figure 2.8. Pipe connections to loading frame on east (a and c) and west (b and d) ends for tens	ion and
cyclic tests	
Figure 3.1. PT44 results for internal pressure, actuator displacement and axial force vs time	18
Figure 3.2. PT44 force vs actuator displacement	18
Figure 3.3. PT44 force vs joint displacement	
Figure 3.4. PT44 axial strains	19
Figure 3.5. PT44 circumferential strains.	
Figure 3.6. Image of PT44 (a) before the start of testing and (b) after failure	19
Figure 3.7. Specimen PT45 results for pressure, axial force, and actuator displacement vs time	20
Figure 3.8. PT45 force vs actuator displacement	21
Figure 3.9. PT45 force vs joint displacements	
Figure 3.10. East and west side for PT45	21
Figure 3.11. Failure at the gasket for PT45	21
Figure 3.12. The spigot after the test	21
Figure 3.13. PT45 axial strains vs time	
Figure 3.14. PT45 circumferential strains vs time	22
Figure 3.15. Specimen PT46 results for pressure, axial force, and actuator displacement vs time	23
Figure 3.16. PT46 force vs actuator displacement	23
Figure 3.17. PT46 force vs joint displacements	23
Figure 3.18. Failure moment at the joint for PT46	24
Figure 3.19. Failure at the west and east sides for PT46	24
Figure 3.20. PT46 axial strains vs time	24
Figure 3.21. PT46 circumferential strains vs time	24
Figure 3.22. Specimen PT50 results for pressure, axial force, and actuator displacement vs time	25
Figure 3.23. PT50 force vs actuator displacement	26
Figure 3.24. PT50 force vs joint displacements	26
Figure 3.25. East and west side for PT50	26
Figure 3.26. Fracture at the spigot for PT50	26
Figure 3.27. PT50 axial strains vs time	27
Figure 3.28. PT50 circumferential strains vs time	27
Figure 3.29. Specimen PT51 results for pressure, axial force, and actuator displacement vs time	28
Figure 3.30. PT51 force vs actuator displacement	28
Figure 3.31. PT51 force vs joint displacements	28
Figure 3.32. Failure moment at joint for PT51	29

College of Engineering and Applied Science 428 UCB Boulder, Colorado 80309-0428

<u>CIEST@colorado.edu</u> website:<u>www.colorado.edu/center/ciest</u>

t: 303.492.8221

Center for Infrastructure, Energy, & Space Testing Boulder, Colorado 80309-

Figure 3.33. Fracture at the spigot for P151	29
Figure 3.34. PT51 axial strains vs time	
Figure 3.35. PT51 circumferential strains vs time	29
Figure 3.36. Specimen PT52 results for pressure, axial force, and actuator displacement vs time	30
Figure 3.37. PT52 force vs actuator displacement	31
Figure 3.38. PT52 force vs joint displacements	31
Figure 3.39. East and west side for PT52	31
Figure 3.40. After failure for PT52	
Figure 3.41. After failure for PT52	31
Figure 3.42. PT52 axial strains vs time	
Figure 3.43. PT52 circumferential strains vs time	32
Figure 3.44. Axial force vs actuator displacement for tension tests	33
Figure 3.45. Axial force vs average joint displacement for tension tests	
Figure 3.46. Axial force vs axial strain for tension tests	34
Figure 3.47. Axial force vs circumferential strain for tension tests	34
Figure 4.1. PS47 results for internal pressure, actuator displacement and axial force vs. time	36
Figure 4.2. PS47 force vs. (a) actuator displacement	36
Figure 4.3. PS47 force vs. joint displacement	36
Figure 4.4. PS47 axial strains vs time	37
Figure 4.5. PS47 circumferential strains vs time	37
Figure 4.6. PS47 joint before testing	37
Figure 4.7. PS47 joint failure	37
Figure 4.8. PS48 results for internal pressure, actuator displacement and axial force vs. time	38
Figure 4.9. PS48 force vs. (a) actuator displacement	39
Figure 4.10. PS48 force vs. joint displacement	39
Figure 4.11. PS48 axial strains vs time	39
Figure 4.12. PS48 circumferential strains vs time	39
Figure 4.13. PS48 joint before testing	40
Figure 4.14. PS48 joint fracture at the west side	40
Figure 4.15. PS49 results for internal pressure, actuator displacement and axial force vs. time	41
Figure 4.16. PS49 force vs. actuator displacement	41
Figure 4.17. PS49 force vs. joint displacement	41
Figure 4.18. PS49 axial strains vs time	42
Figure 4.19. PS49 circumferential strains vs time	42
Figure 4.20. PS49 joint before testing	42
Figure 4.21. PS49 joint failure	42
Figure 4.22. PS53 results for internal pressure, actuator displacement and axial force vs. time	43
Figure 4.23. PS53 force vs. actuator displacement	44
Figure 4.24. PS53 force vs. joint displacement	44
Figure 4.25. PS53 axial strains vs time	45
Figure 4.26. PS53 circumferential strains vs time	45
Figure 4.27. PS53 failure moment (The close-up view of North side)	45
Figure 4.28. PS53 fracture at the bell side of the joint (The close-up view of South side)	45
Figure 4.29. The cyclic loading sequence for PS54	46

College of Engineering and Applied Science 428 UCB Boulder, Colorado 80309-0428

t: 303.492.8221 CIEST@colorado.edu website:www.colorado.edu/center/ciest

Center for Infrastructure, Energy, & Space Testing Boulder, Co

Figure 4.30. PS54 results for internal pressure, actuator displacement and axial force vs. time	47
Figure 4.31. PS54 force vs. actuator displacement	48
Figure 4.32. PS54 force vs. joint displacement	48
Figure 4.33. PS54 axial strains vs time	48
Figure 4.34. PS54 circumferential strains vs time	48
Figure 4.35. PS54 joint before testing	49
Figure 4.36. PS54 joint failure	49
Figure 4.37. The cyclic loading sequence for PS55	50
Figure 4.38. PS55 results for internal pressure, actuator displacement and axial force vs. time	50
Figure 4.39. PS55 force vs. actuator displacement	51
Figure 4.40. PS55 force vs. joint displacement	51
Figure 4.41. PS55 axial strains vs time	51
Figure 4.42. PS55 circumferential strains vs time	51
Figure 4.43. PS55 joint before testing	52
Figure 4.44. PS55 joint failure due to fracture on the spigot	52
Figure 4.45. Cyclic comparison - force vs. actuator displacement	53
Figure 4.46. Cyclic comparison - force vs. average joint displacement	53
Figure 4.47. Cyclic comparison - force vs. joint displacement	53
Figure 4.48 Cyclic comparison - force vs. axial strain	54



College of Engineering and Applied Science 428 UCB Boulder, Colorado 80309-0428

t: 303.492.8221 CIEST@colorado.edu

website: www.colorado.edu/center/ciest

List of Tables

Table 1.1. Summary of Axial Tests and Specimens (all tests included RieberLok Gask	ets and were tested
at a target internal pressure of 65 psi (448 kPa)	9
Table 2.1. The loading sequence for a) LP1 and b) LP2	16
Table 3.1. Summary of tension test results	33
Table 4.1. Summary of cyclic test results	53

College of Engineering and Applied Science 428 UCB

CIEST@colorado.edu website: www.colorado.edu/center/ciest

t: 303.492.8221

Boulder, Colorado 80309-0428

1. Introduction

This report is submitted to Northern Pipe Product Inc., Fargo, ND, and presents test results from a program to investigate the axial performance of nominal 6-in. (150-mm) diameter polyvinyl chloride (PVC) pipe and joints with reinforced gaskets. The components tested included VinylTech and Northern PVC pipes with bell and spigot connections fitted with RieberLok Gaskets. The work was undertaken in the Center for Infrastructure, Energy, and Space Testing (CIEST) which is affiliated with the Civil, Architectural, and

Environmental Engineering Department at the University of Colorado Boulder.

The intention of this study is to provide axial test results for PVC pipes made from two different factories and paired with RieberLok gaskets. In addition, the results of the axial tension and cyclic tests can assist in understanding external and internal loading conditions that a pipeline system may experience during significant ground deformations that are possible during earthquake-induced land sliding, fault rupture, and liquefaction-induced lateral spreading, thus characterizing the pipeline system capacity. As detailed, all tests were designed and performed in accordance with procedures and recommendations provided by Wham et al. (2018 & 2019) as well as the ASCE Standard Seismic Testing and Evaluation of Pipelines Systems

(STEPS) currently under development.

This report is organized into five sections. Section 1 provides introductory remarks, Section 2 provides discussion of the test specimen and experimental overview. Sections 3 and Section 4 provide a discussion of axial tension, and axial cyclic tests respectively. Concluding remarks are presented in Section 5.

Appendix A presents detailed information related to strain gauge application.

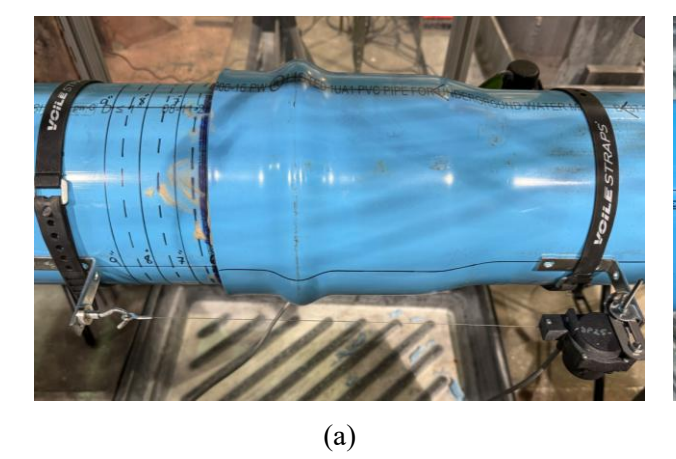
1.1 Test Specimens

Pipe specimens consist of C900 polyvinyl chloride (PVC), Pressure Class 235, and DR18 pipe manufactured by Northern Pipes and VinylTech. The connections under investigation are the bell-andspigot joint with the RieberLok gasket for all PVC pipes (Figure 1.1). The PVC pipes manufactured by Northern Pipe and VinylTech have the same nominal diameter (6 in.), outside diameter (6.90 in.), and wall thickness (0.383 in.). The RieberLok gasket has a total of 15 teeth in the shape of five groups, as shown in

Figure 2.6.

College of Engineering and Applied Science 428 UCB Boulder, Colorado 80309-0428 t: 303.492.8221 CIEST@colorado.edu website:www.colorado.edu/center/ciest

Center for Infrastructure, Energy, & Space Testing



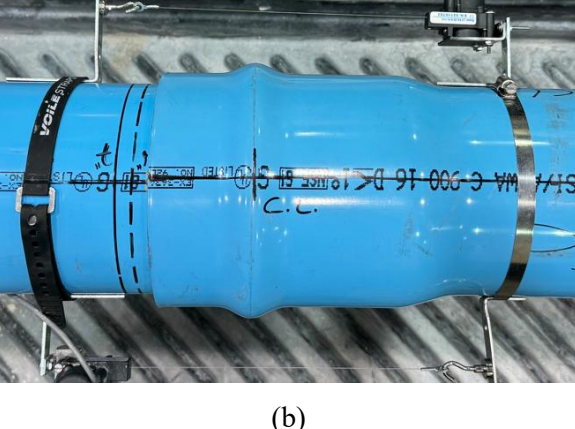


Figure 1.1. Example of a typical bell/spigot joint for a) Northern Pipe and b) VinylTech

1.2 Test Overview

All specimens tested herein are 6-in (150-mm) diameter pipe, 235 Pressure Class (DR18), commercially available and conforming to C900 (PVC) standards. Table 1.1 provides an overview of the axial test (Tension and Cyclic) specimens and experiments performed. The Test ID represents the test type and a unique numerical value specific to the sequence of all testing performed at CIEST. Joint Type identifies the pipe material connection type while Internal Pressure classifies the approximate internal water pressure at which each test is conducted.

Table 1.1. Summary of Axial Tests and Specimens (all tests included RieberLok Gaskets and were tested at a target internal pressure of 65 psi (448 kPa)

Test ID	Test Type	Pipe Type (Company)			
PT44	Axial Tension	(VinylTech)	65 [448]	1	
PT45	Axial Tension	(VinylTech)	65 [448]	1	
PT46	Axial Tension	(VinylTech)	65 [448]	1	
PS47	Axial Cyclic	(VinylTech)	65 [448]	1	
PS48	Axial Cyclic	(VinylTech)	65 [448]	1	
PS49	Axial Cyclic	(VinylTech)	65 [448]	1	
PT50	Axial Tension	(Northern)	65 [448]	2	
PT51	Axial Tension	(Northern)	65 [448]	2	
PT52	Axial Tension	(Northern)	65 [448]	2	
PS53	Axial Cyclic	(Northern)	65 [448]	2	
PS54	Axial Cyclic	(Northern)	65 [448]	2	
PS55	Axial Cyclic	(Northern)	65 [448]	2	

College of Engineering and Applied Science 428 UCB

Boulder, Colorado 80309-0428

<u>CIEST@colorado.edu</u> website:<u>www.colorado.edu/center/ciest</u>

t: 303.492.8221

2. Axial Testing

This section provides a detailed overview of the setup procedure and key experimental constraints associated with application of axial load to water distribution pipelines. The objective is to expose the system to external loading conditions representative of the significant deformations that can be caused during earthquake-induced ground motions to characterize the pipeline system capacity. All tests are designed and performed in accordance with procedures and recommendations provided by Wham et al. (2018 & 2019) and additional details about the setup are provided by Ihnotic (2019).

2.1 Axial Test Setup

This section outlines the test setup procedure for axial loading of a given pipe specimen. Figure 2.1 and Figure 2.2 shows images of the axial test setup and equipment for two different test frames (frame 1 and frame 2). Frame 1 is equipped with a 244.41 MTS actuator with a 110-kip (490-kN) load cell and a 10-inch (245 mm) displacement capacity. Frame 2 is equipped with a 244.51 MTS actuator with a 220-kip (980-kN) load cell and a 12-inch (260 mm) displacement capacity. Figure 2.3 and Figure 2.4 show the dimensioned drawings of frame 1 and frame 2, respectively.



Figure 2.1. Axial test setup in the loading frame 1

College of Engineering and Applied Science 428 UCB Boulder, Colorado 80309-0428

t: 303.492.8221 CIEST@colorado.edu website:www.colorado.edu/center/ciest

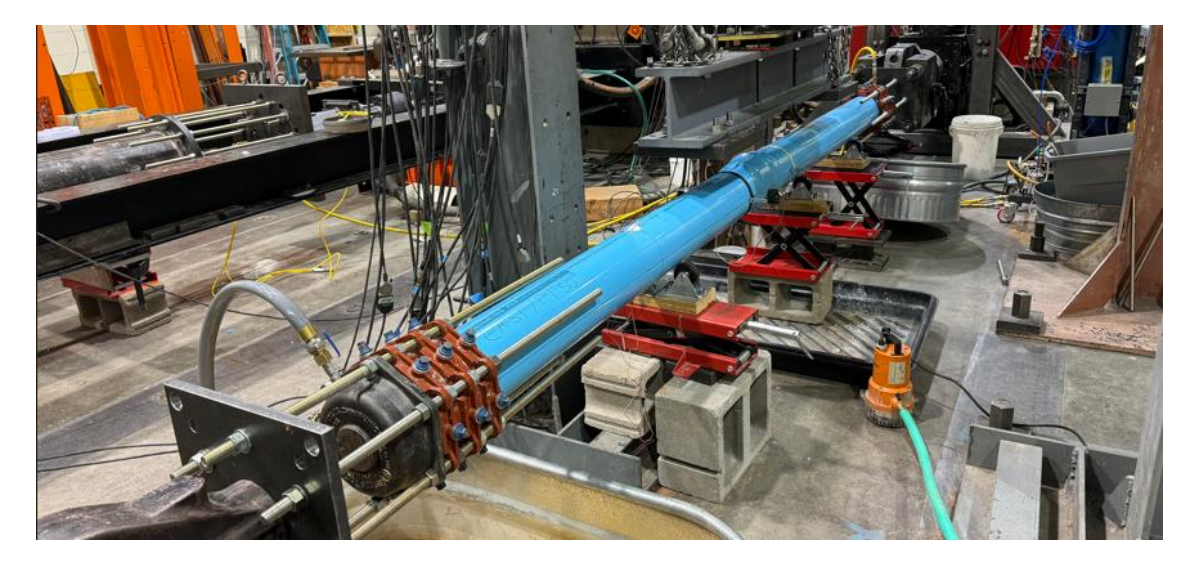


Figure 2.2. Axial test setup in the loading frame 2

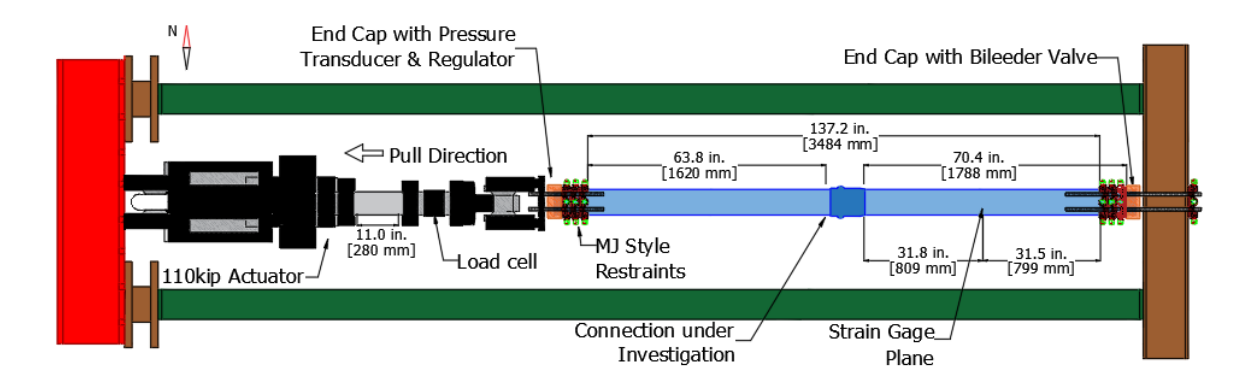


Figure 2.3. Dimensioned drawing of axial test setup for frame 1

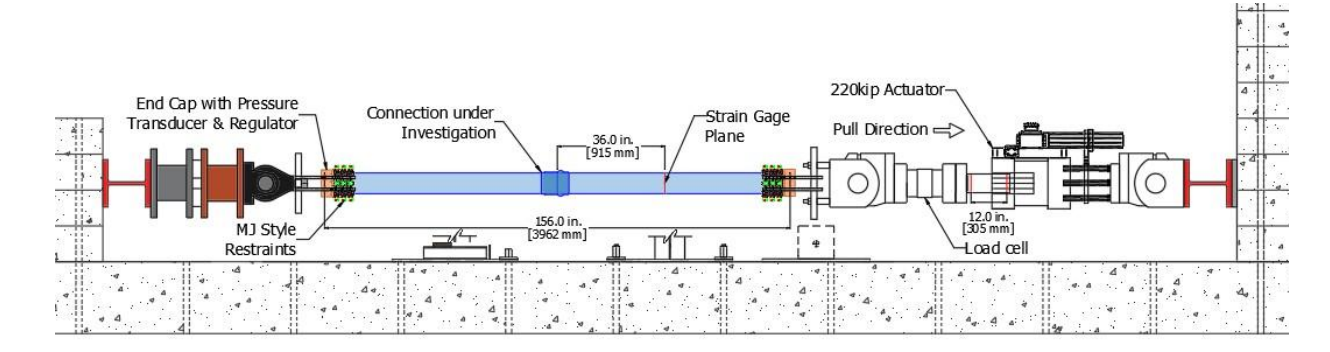


Figure 2.4. Dimensioned drawing of axial test setup for frame 2

College of Engineering and Applied Science 428 UCB

Boulder, Colorado 80309-0428

<u>CIEST@colorado.edu</u> website:<u>www.colorado.edu/center/ciest</u>

t: 303.492.8221

2.1.1 Specimen Installation Procedure

The pipe specimens are prepared at a length of approximately 13 ft (3.96 m) and 14 ft (4.26 m) for tensile testing; consisting of two 78-in. (1980-mm) and cyclic test; consisting of two 84-in. (2130 mm) segments, respectively. The length varies depending on the loading direction (tension or cyclic) and connection under investigation. The pipe is cut using standard field installation practices. Measurements are provided at 0.5 in (13 mm) increments on the pipe joints (along the spigot), as shown in Figure 2.5. A level and crowning tool are used to identify the crown(top), invert(bottom), and spring lines(sides) of the pipe. The strain gage plane is marked at 36 in (900 mm) from the east side (bell) of the specimen center line. The RieberLok gasket was installed, as shown in Figure 2.6. Figure 2.7 shows the connection prior to joint insertion.



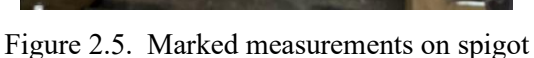




Figure 2.6. Installation of RieberLok gasket



Figure 2.7. Bell and spigot before joint insertion

Three and four 2006PV Megalug external restraints are used at either end of the specimen to transfer externally applied axial load for tension and cyclic tests, respectively. Figure 2.8 shows the restraints positioned at the loading end (west) and fixed end (east) of the specimens. The outer most restraint for each end is aligned 1.5 in. (38 mm) from the end pipe and hand tightened into place. Each set of restraints are aligned with their perspective end loading arrangements. The east side, fixed to the load frame, is positioned with a threaded rod located at the crown of the specimen, and the west side (actuator or loading side) is aligned with restraint nuts located at the crown. Two short threaded rods are used to pull the remaining two restraints into contact with the first. The clamping nuts of the remaining Megalugs are hand tightened into place.

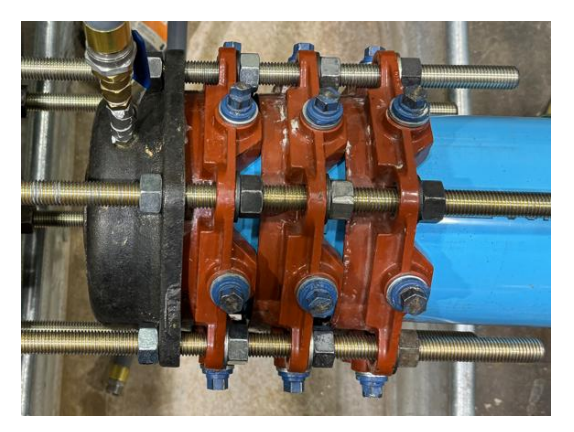
College of Engineering and Applied Science 428 UCB

t: 303.492.8221 CIEST@colorado.edu

website:www.colorado.edu/center/ciest

The nuts on each end restraint are tightened using a torque wrench set to 20 ft-lb (27.1 N-m). The nuts are tightened in a star pattern to 60 ft-lb (81.3 N-m) in steps of 20 ft-lb. The process is repeated until all restraints are secured to the pipe. While the Megalug restraint is equipped with self-torquing, twist off clamping nuts for typical field installation, prior experience suggests the incrementally increasing torque wrench provides

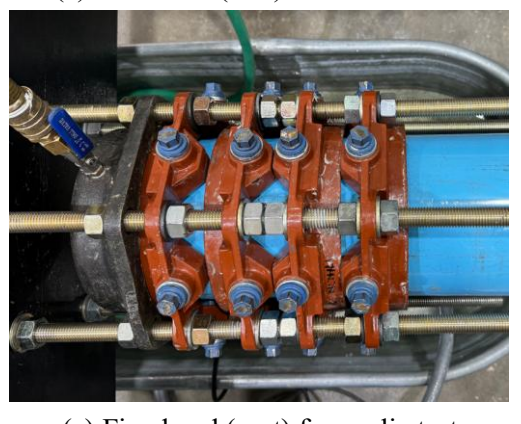
Boulder, Colorado 80309-0428



(a) Fixed end (east) for tension test



(b) Loading end (west) for tension test



(c) Fixed end (east) for cyclic test



(d) Loading end (west) for cyclic test

Figure 2.8. Pipe connections to loading frame on east (a and c) and west (b and d) ends for tension and cyclic tests

a uniformly distributed clamping force that ensures uniform circumferential contact and deters failure at the ends of the specimen.

Strain Gauges are installed at designated locations following the procedure outlined in "Strain Gauge Application Procedure" (Appendix A) and additional details are included in the following section.

The specimen is placed in the loading frame and the east and west connections are appropriately aligned with the actuator in its full extended position (tension test) or centered position (cyclic test). Lubrication

University of Colorado Boulder

Center for Infrastructure, Energy, & Space Testing

College of Engineering and Applied Science 428 UCB

Boulder, Colorado 80309-0428

t: 303.492.8221 CIEST@colorado.edu

<u>CIEST@colorado.edu</u> website:<u>www.colorado.edu/center/ciest</u>

(necessary for the gasket) is applied to the endcap gaskets and the inner diameter of the endcaps, the gasket is positioned against the outermost end restraint, and the endcaps tightened in place with threaded rods (Figure 2.8). The west end cap is equipped with pressurization equipment and water inlet while the east endcap includes a bleeder valve at the crown to remove air during filling of the pipe. The hose for the water intake on the west endcap and the air release valve on the east endcap are positioned vertically. Two short threaded rods on the crown and the invert (east) and on each spring line (west) are installed to secure the endcap to the pipe. On the east end, six 36-in (900 mm) long, 0.75-in (19 mm) diameter high-strength (120 ksi) threaded rods are installed to secure the pipe to the frame. Nuts and washers are then applied to each end to secure the pipe to the testing frame. A similar procedure is followed on the east end. The steel nuts and threaded rod connections are arranged such that axial force from pressurization is resisted by the actuator, and thus recorded by the actuator load cell.

2.1.2 Instrumentation

Two string potentiometers (string pots) are attached to the specimen at the joint to measure joint axial displacements. An electronic pressure transducer (PPT) is installed on the west end to measure internal water pressure during testing.

Two x-y pair strain gauges are fixed to the exterior of the specimen at the strain gauge plane. The plane locations are positioned approximately halfway between the joint restraint (specimen centerline) and end restraints. The strain gauges are placed at the crown and invert. Gauge plane SG+36 is positioned 36 in. (900 mm) east of the specimen centerline and includes two x-y gauges, oriented in the axial and circumferential direction.

2.2 Axial Test Procedure

The following section provides details of the overall test sequence separated into three parts: pretest, test sequence, and discussion of pause or stop criteria.

2.2.1 Pretest

Once the specimen is secured in the loading frame and the calibrated instrumentation is installed, the measuring systems are verified. The pipe is filled with water with the air bleed in the open position. The air bleed is closed once water has streamed from it and the system is pressurized to the laboratory pressure of approximately 65 psi (448 kPa) to check for leaks. Water is introduced into the specimen more than five hours before testing to ensure thermal acclimation to ambient laboratory conditions. Temperature readings of the external wall of the pipe are taken at several locations. Multiple pressurization sequences are

University of Colorado Boulder

College of Engineering and Applied Science 428 UCB

t: 303.492.8221 CIEST@colorado.edu

Center for Infrastructure, Energy, & Space Testing Boulder, Colorado 80309-0428

website:www.colorado.edu/center/ciest

completed to seat gaskets, verify readings of strain gauges, and check axial force measured by the load cell. In each of the cycles, the air bleed valve is opened to release any accumulating air. Prior to a pressurization sequence, the nuts between the loading frame and the endcaps are tightened, such that when the pipe is pressurized, the axial pressurization force can be measured by the load cell. During the pressurization sequences, the pipe is pressurized to approximately 65 psi (448 kPa) and back down to 0 psi several times. After each sequence, data was collected, stored, and analyzed to ensure proper function of all measuring systems. The area surrounding the testing frame is cleared of all tools and other objects. Once ready for the test, a pretest meeting is conducted to review installation conditions, walk through instrumentation locations and expectations, and discuss safety equipment and concerns.

2.2.2 Tension Test Sequence

After the pretest meeting is conducted and roles assigned, the test sequence is initiated by starting the data acquisition system and laboratory hydraulic systems. A data sampling rate of 4 Hz was used for all reported tests. The loading nuts at either end of the specimen are checked to avoid any end movement due to pressurization. The appropriate water pressure is applied depending on the specific test. The test is performed under displacement control at a rate of 1 in. per minute. Displacement was applied until the specimen is no longer capable of holding internal water pressure or until reaching the maximum stroke of the actuator. Once the test is completed, the data acquisition system is turned off, laboratory hydraulic systems set to low pressure, and data is backed up.

2.2.3 Cyclic Test Sequence

For each cyclic test, a series of tensile and compressive loads were applied to the pipe specimen with increasing amounts of displacement. Cyclic loading was applied according to the guidelines of FEMA461, which discusses seismic loading protocols for structural and non-structural building components (Applied Technology Council (ATC), 2007). Two different loading protocols were conducted for all axial cyclic tests. Table 2.1a shows the first cyclic loading protocol used in PS47. Table 2.1b shows the second cyclic loading protocol used in other five cyclic tests. Each cycle began with loading in the tensile direction. The displacements shown are measured from the "zero" point established at the beginning of the test. After cyclic loading, the specimen was loaded in tension to failure. All loads were applied at a displacement rate of 1 in. (25 mm) per minute except for PS54. The loads were applied at a displacement rate of 9 in. (228 mm) per minute for PS54.

College of Engineering and Applied Science 428 UCB

 $\underline{\text{CIEST@colorado.edu}}$ website: $\underline{\text{www.colorado.edu/center/ciest}}$

t: 303.492.8221

Center for Infrastructure, Energy, & Space Testing

Table 2.1. The loading sequence for a) LP1 and b) LP2

Boulder, Colorado 80309-0428

	(a)	
Step	Inches	Cycles
1	0.0192	2 Cycles
2	-0.0192	2 Cycles
3	0.0269	2 Cycles
4	-0.0269	2 Cycles
5	0.0376	2 Cycles
6	-0.0376	2 Cycles
7	0.0527	2 Cyalas
8	-0.0527	2 Cycles
9	0.0738	2 Cyalas
10	-0.0738	2 Cycles
11	0.1033	2 Cycles
12	-0.1033	2 Cycles
13	0.1446	2 Cycles
14	-0.1446	2 Cycles
15	0.2024	2 Cycles
16	-0.2024	2 Cycles
17	0.2834	2 Cyalas
18	-0.2834	2 Cycles
19	0.3967	2 Cyalas
20	-0.3967	2 Cycles
21	Tension U	ntil Failure

	(b)			
Step	Inches	Cycles		
1	0.0403	2 Cycles		
2	-0.0403	2 Cycles		
3	0.0564	2 Cycles		
4	-0.0564	2 Cycles		
5	0.079	2 Cycles		
6	-0.079	2 Cycles		
7	0.1106	2 Cycles		
8	-0.1106	2 Cycles		
9	0.1549	2 Cycles		
10	-0.1549	2 Cycles		
11	0.2169	2 Cycles		
12	-0.2169	2 Cycles		
13	0.3036	2 Cycles		
14	-0.3036	2 Cycles		
15	0.425	2 Cycles		
16	-0.425	2 Cycles		
17	0.595	2.01		
18	-0.595	2 Cycles		
19	0.8331	2 Cycles		
20	-0.8331	2 Cycles		
21 Tension Until Failure				

2.2.4 Stop or Pause Criteria

Several predetermined interruptions to the test sequence are identified before testing. The test is paused if the specimen loses water pressure during the test. If undesirable leakage occurs at the end caps they are tightened, and the test is resumed. If any leakage is observed at the coupling or center of the specimen (serviceability limit state), the test is paused briefly, leakage rate assessed, and the test resumed until ultimate failure. The test is paused if any fundamental instrumentation malfunctions during the test, or if power is lost in any part of the testing laboratory. The test is terminated when the specimen is unable to hold internal water pressure, which typically occurs as a result of structural failure of the pipe body or connection.

College of Engineering and Applied Science 428 UCB Boulder, Colorado 80309-0428

<u>CIEST@colorado.edu</u> website:<u>www.colorado.edu/center/ciest</u>

t: 303.492.8221

3. Axial Tension Test Results

The following section provides results from axial tension tests performed on the Northern and VinylTech pipe with Rieber bell shape. A total of six axial tension tests are reported in the following sections. For all tests, displacement was applied at a rate of 1 in. (25 mm) per minute. The common procedure and the same gasket were used for all axial tension tests.

3.1 Tension Test (PT44)

Figure 3.1 also shows the actuator force, applied displacement, and internal pressure relative to time during test PT44. As shown by the blue line in Figure 3.1, water pressure was held relatively constant at ~65 psi (448 kPa) for the duration of the loading. The slight fluctuations in pressure are a function of the increasing internal volume during applied tensile loading. Figure 3.2 shows the relationship between the actuator force and actuator displacement. Actuator forces and displacements are direct measurements of the hydraulic load cell and piston, respectively. The maximum force recorded in the load cell of the actuator was 26.3 kips (116.8 kN) and the maximum applied displacement was 2.39 in. (60.70 mm). Figure 3.3 shows the actuator force vs the joint displacement. At the maximum applied force, the joint reached an average displacement of 0.79 in. (20.06 mm) while the maximum joint displacement prior to failure was ~1 in. (25.4 mm).

Images of bell-and-spigot connection before and after the test are shown in Figure 3.6. The dot marks are for digital image correlation (DIC) measurement on the white surface. While the DIC measurements captured 3D displacement and strain fields that correlated well with standard measurement techniques, this measurement technique is beyond this project report scope. Joint displacement was measured using two string potentiometers located 3 in. (75 mm) away from the joint on both ends of the coupling, shown in Figure 3.6 (a). The reported joint displacement does include the elongation of the pipe barrel over 3 inches (75 mm) on either side of the joint, which is practically negligible compared to the displacement between bell and spigot in these tests. Failure occurred on the West side (spigot) of the bell-and-spigot connection. Fracture occurred in the spigot section of pipe at the location where the gasket teeth penetrated into the pipe barrel, as shown in Figure 3.6 (b).

College of Engineering and Applied Science 428 UCB

t: 303.492.8221 <u>CIEST@colorado.edu</u> website:<u>www.colorado.edu/center/ciest</u>

Center for Infrastructure, Energy, & Space Testing Boulder, Colorado 80309-0428

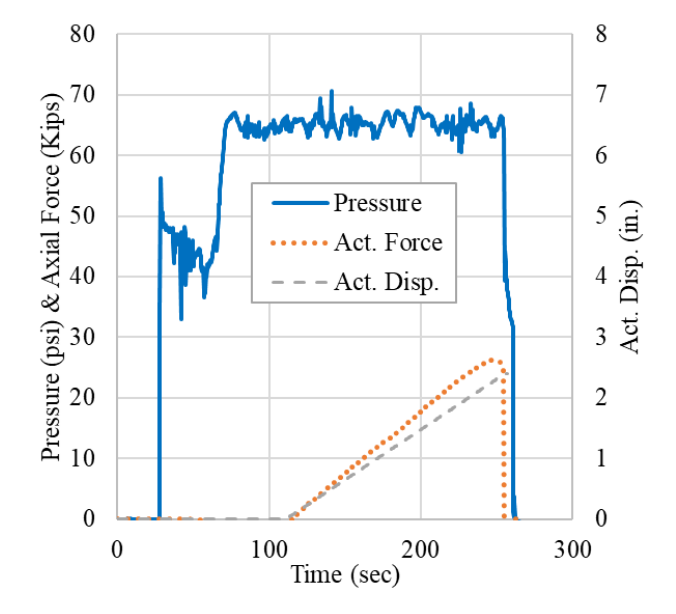


Figure 3.1. PT44 results for internal pressure, actuator displacement and axial force vs time

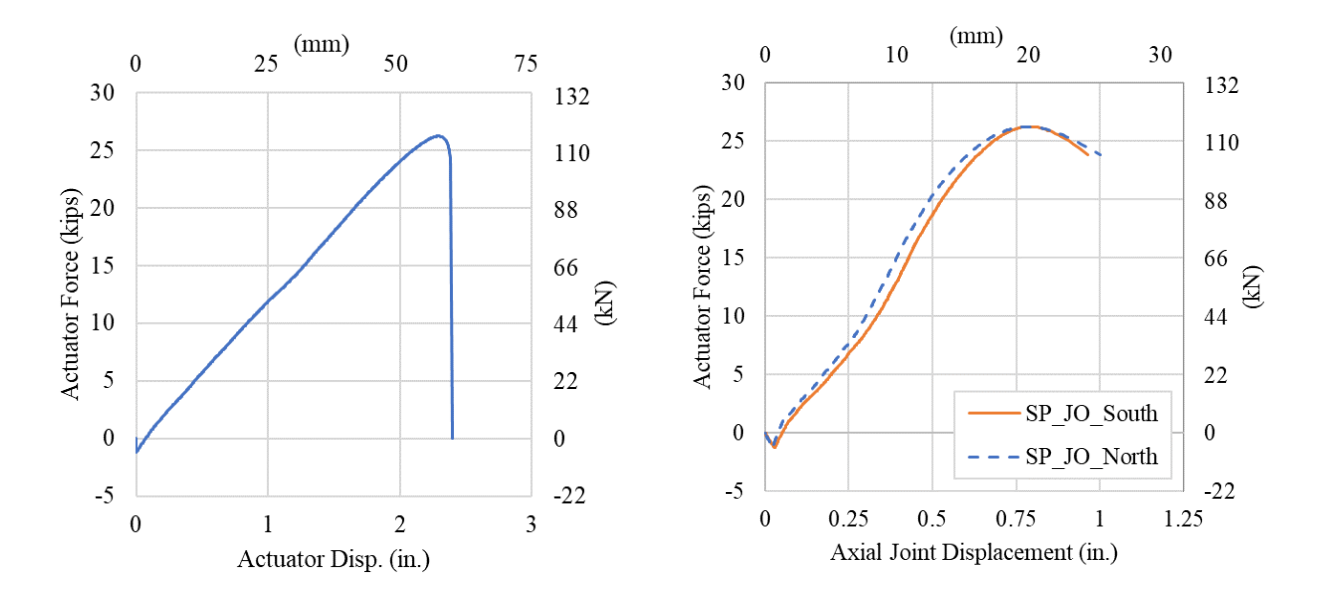


Figure 3.2. PT44 force vs actuator displacement

Figure 3.3. PT44 force vs joint displacement

Figure 3.4 and 3.5 shows the axial and circumferential strains measured at a plane 36 in (910 mm) away from the center line (middle of the joint) for the duration of the test, respectively. Strain gauges were placed at the crown and invert positions. At approximately 75 seconds the system was pressurized, and an increase in circumferential strain and a slight decrease in axial strain were observed. Once loading began (t=115 sec), the circumferential strains began to decrease, while the axial strains increased. As the actuator applied tensile loading to the system, the pipe began to elongate, causing an increase in axial strains. Due to



College of Engineering and Applied Science 428 UCB Boulder, Colorado 80309-0428

t: 303.492.8221 CIEST@colorado.edu

website:www.colorado.edu/center/ciest

Poisson's effect, the circumferential strain decreased as the tensile load was applied. The maximum axial strain and circumferential strain were measured at about 0.82% and - 0.21% prior to failure, respectively.

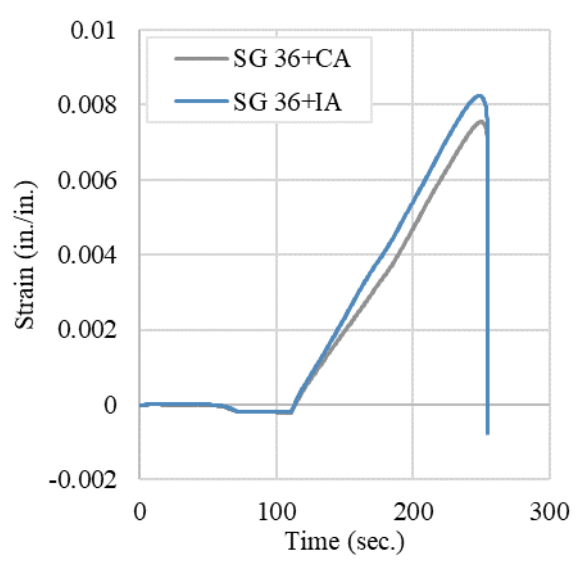


Figure 3.4. PT44 axial strains

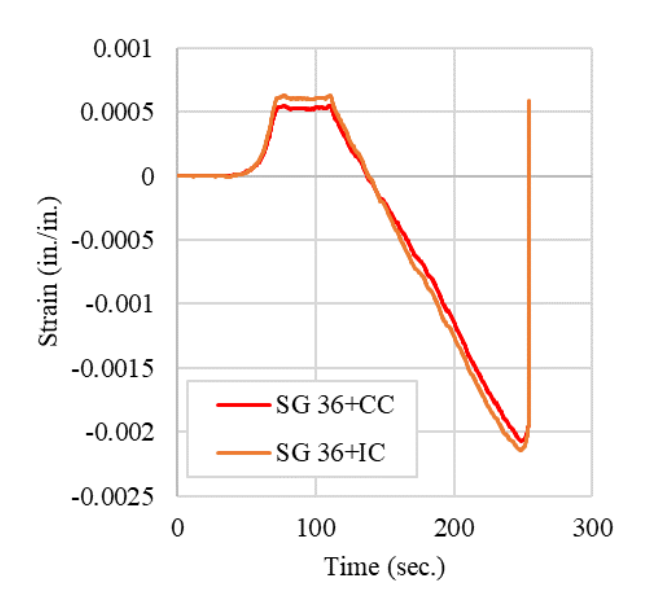


Figure 3.5. PT44 circumferential strains.

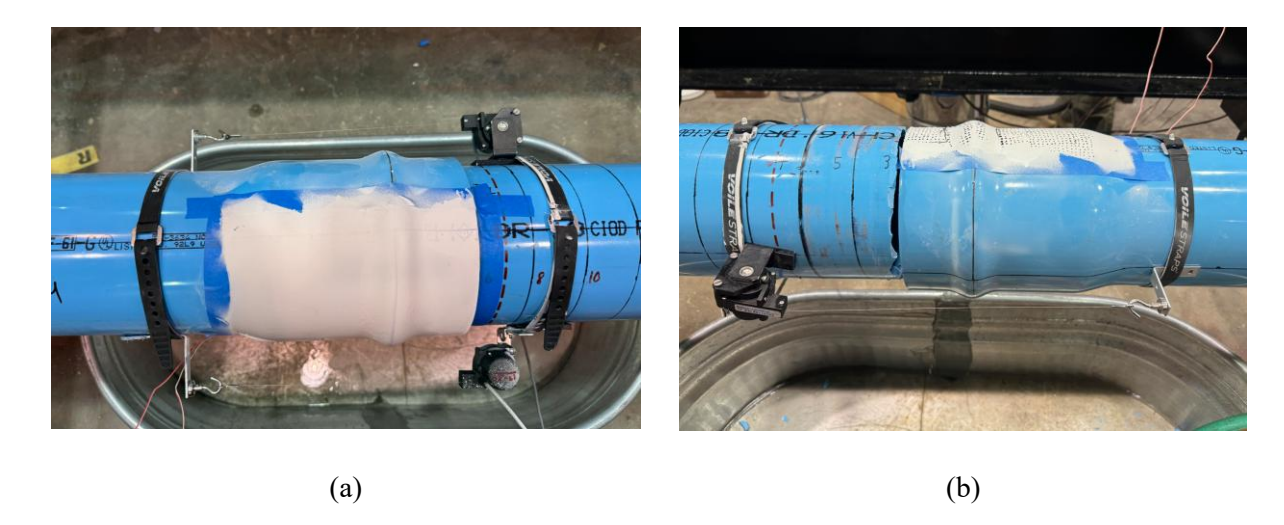


Figure 3.6. Image of PT44 (a) before the start of testing and (b) after failure

College of Engineering and Applied Science 428 UCB Boulder, Colorado 80309-0428 t: 303.492.8221 CIEST@colorado.edu website:www.colorado.edu/center/ciest

Center for Infrastructure, Energy, & Space Testing

3.2 Tension Test (PT45)

The material and instrumentation used for this test were consistent with the previous test (PT44). Figure 3.7 shows the relationship among actuator force, internal pressure, and actuator displacement relative to time. A constant internal water pressure of 63 ± 2 psi $(434 \pm 13 \text{ kPa})$ was provided during the test. At t=120 sec, displacement was applied at a rate of 1.0 in./min. (25 mm/min.), and the force feedback of the load cell was recorded. When the specimen lost its force capacity (t=260 sec), the pressure dropped to about 30 psi and then increased again to 65 psi (448 kPa). After pausing to confirm the capacity of the specimen to sustain the target internal pressure, application of axial displacement was continued. At an applied axial displacement of a substantial leak occurred as the spigot pulled out of the bell and the specimen lost pressure integrity. Figure 3.8 shows that the maximum force recorded in the load cell was 25.9 kips (115.3 kN) at an actuator displacement of 2.25 in. (57.2 mm). Figure 3.9 shows the actuator force relative to joint displacement. Joint displacement was measured using two string pots located on the north and south spring lines of the specimen as shown in Figure 3.10. The joint displacement reached an average of about 0.8 in. (20.3 mm) at the maximum force and reached a total of about 0.99 in (25.1 mm) just before failure (23.0 kips). Figure 3.11 shows damage to the gasket post-test, where several of the metal teeth were deformed, reducing the force capacity of the joint, but allowing the gasket to continue to provide containment after the force dropped. Figure 3.12 shows marks of the metal teeth on spigot after the test.

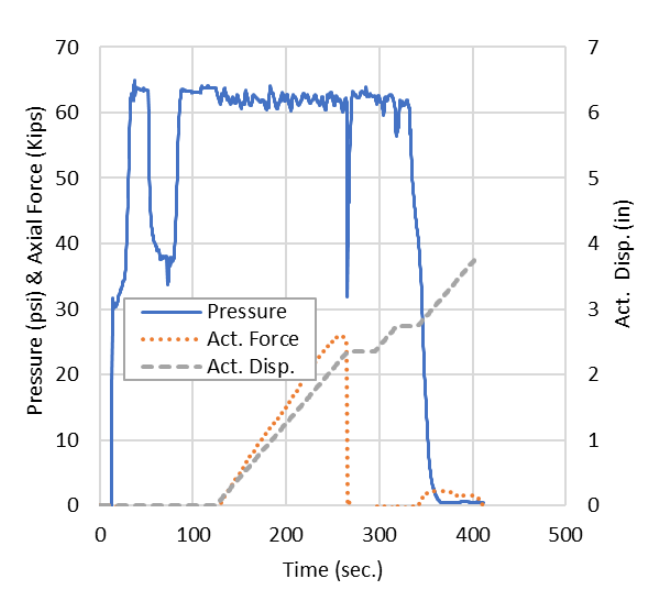


Figure 3.7. Specimen PT45 results for pressure, axial force, and actuator displacement vs time

Boulder

College of Engineering and Applied Science
428 UCB
Boulder, Colorado 80309-0428

t: 303.492.8221 CIEST@colorado.edu

website:www.colorado.edu/center/ciest

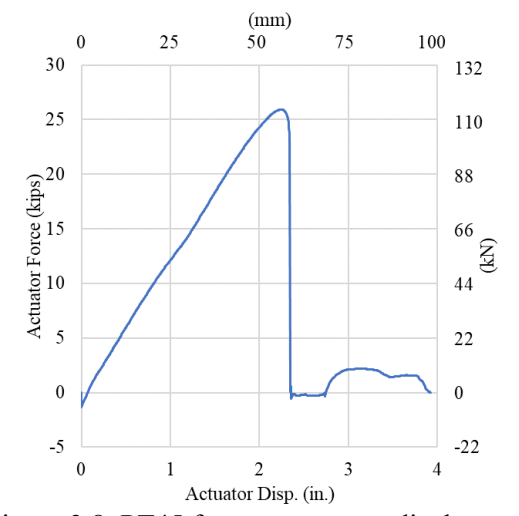


Figure 3.8. PT45 force vs actuator displacement

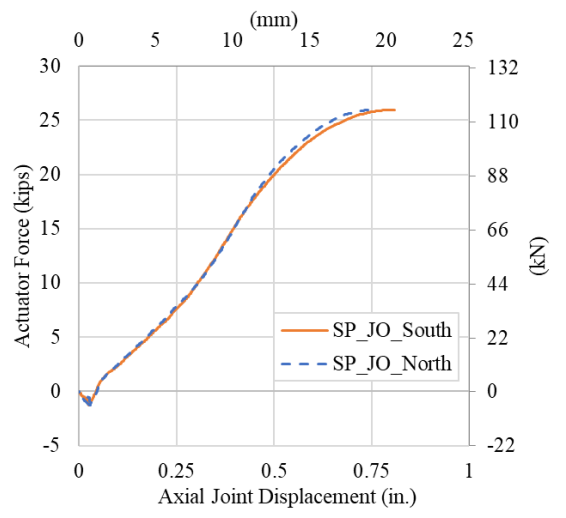


Figure 3.9. PT45 force vs joint displacements

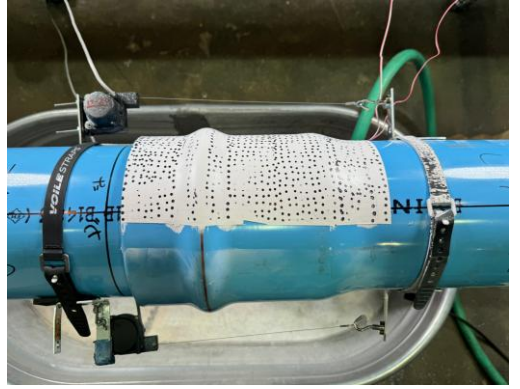






Figure 3.10. East and west side for PT45

Figure 3.11. Failure at the gasket for PT45

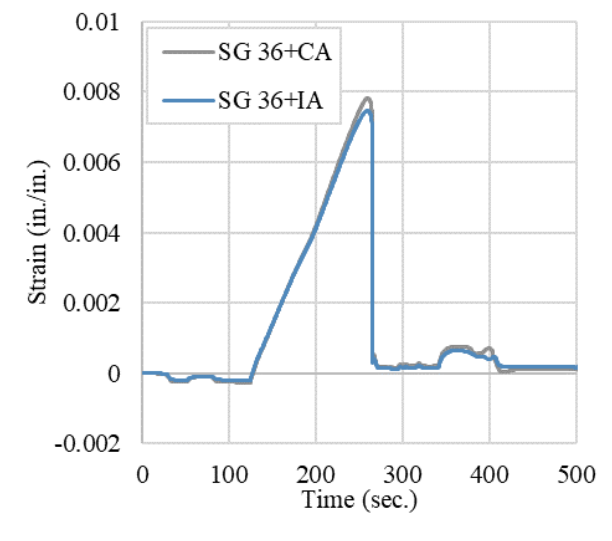
Figure 3.12. The spigot after the test

Figure 3.13 and Figure 3.14 show the axial and circumferential strains, respectively, measured at a plane 36 in (910 mm) away from the center line for the duration of the test. The system was fully pressurized and an increase in circumferential strain was observed at the beginning of the test. After the start of loading, the circumferential strains decreased while the axial strains increased. Under the influence of the actuator tensile loading on the system, the pipe began to elongate, resulting in a rise in axial strains. Concurrently, Poisson's effect caused a reduction in circumferential strain as the tensile load was imposed. The maximum axial strain and circumferential strain were measured at about 0.78% and -0.22% before failure, respectively.

College of Engineering and Applied Science 428 UCB

t: 303.492.8221 <u>CIEST@colorado.edu</u> website:<u>www.colorado.edu/center/ciest</u>

Center for Infrastructure, Energy, & Space Testing Boulder, Colorado 80309-0428



0.001 0.0005 0 Strain (in./in.) -0.0005 -0.001 -0.0015 SG 36+CC -0.002 SG 36+IC -0.00250 100 300 500 200 400 Time (sec.)

Figure 3.13. PT45 axial strains vs time

Figure 3.14. PT45 circumferential strains vs time

3.3 Tension Test (PT46)

The third tension test performed on PVC pipe manufactured by VnyilTech was PT46. Figure 3.15 shows the relationship between actuator force, internal pressure, and actuator displacement relative to time. Displacement was applied at a rate of 1.0 in./min. (25 mm/min.), and the force feedback of the load cell was recorded. Figure 3.16 shows that the maximum force recorded in the load cell was 27.6 kips (122.7 kN) at an actuator displacement of 2.36 in. (59.9 mm). A constant internal water pressure of 65 ± 2 psi (448 ± 13 kPa) was applied. Figure 3.17 shows the actuator force vs the joint displacement. The joint displacement reached an average of about 0.8 in. (20.32 mm) just before failure. Figure 3.18 shows failure moment at the joint. Fracture occurred on the east and west sides of the joint at the maximum force (27.6 kips). The circumferential fracture occurred where the teeth of the gasket penetrate the spigot. On the bell side, a fracture occurred at an angle of almost 45 degrees, starting from the crown and reaching the inverts, as shown in Figure 3.19.

College of Engineering and Applied Science 428 UCB

Boulder, Colorado 80309-0428

t: 303.492.8221 CIEST@colorado.edu

Center for Infrastructure, Energy, & Space Testing

website:www.colorado.edu/center/ciest

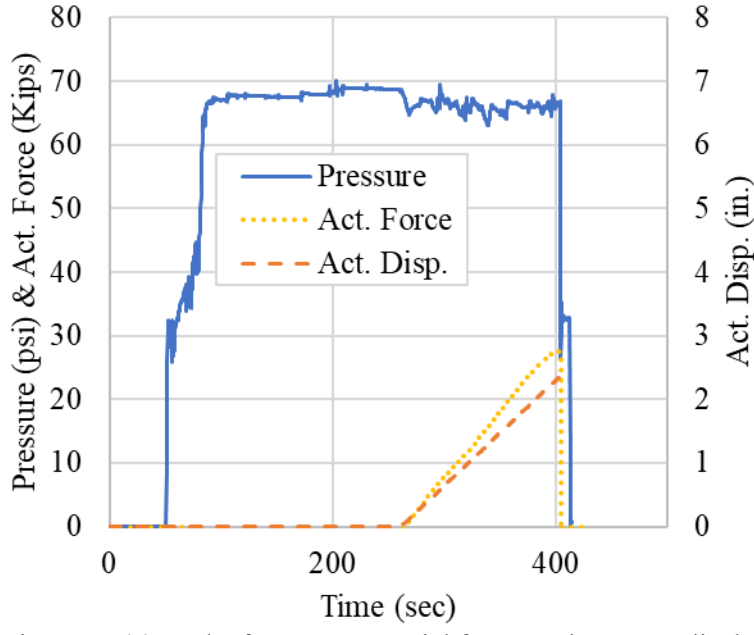


Figure 3.15. Specimen PT46 results for pressure, axial force, and actuator displacement vs time

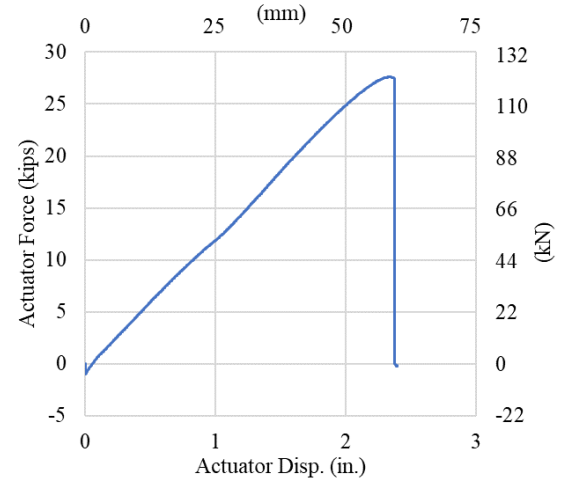


Figure 3.16. PT46 force vs actuator displacement

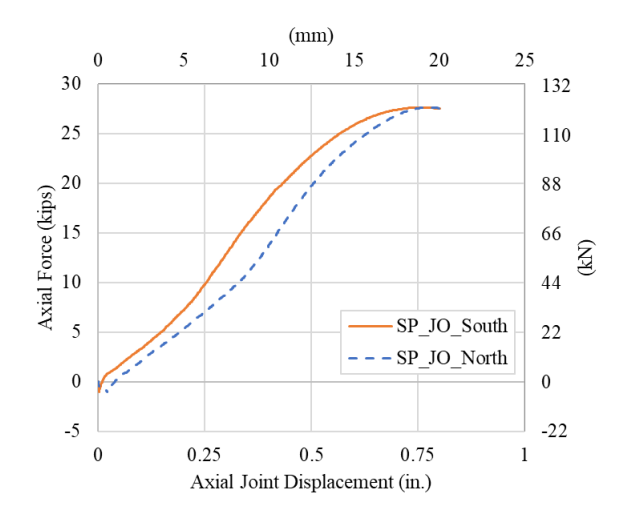


Figure 3.17. PT46 force vs joint displacements

Center for Infrastructure, Energy, & Space Testing Boulder, Co

428 UCB
Boulder, Colorado 80309-0428

Website: www.colorado.edu/center/ciest





Figure 3.18. Failure moment at the joint for PT46

Figure 3.19. Failure at the west and east sides for PT46

Figure 3.20 and Figure 3.21 shows the average axial and circumferential strains for the duration of the test. At the start of the test, the system was fully pressurized, and an increase in circumferential strain was observed. Once loading began, the circumferential strains began to decrease, while the axial strains increased. As the actuator applied tensile loading to the system, the pipe began to elongate, causing an increase in axial strains. Due to Poisson's effect, the circumferential strain decreased as the tensile load was applied. The maximum axial strain and circumferential strain were measured at about 0.81% and -0.22% before failure, respectively.

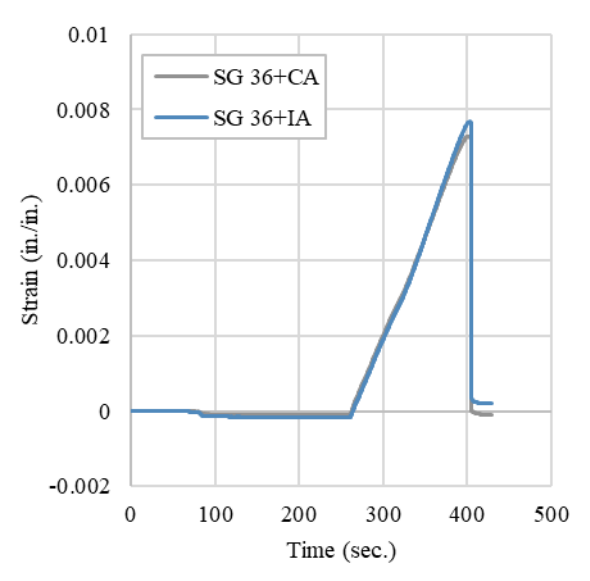


Figure 3.20. PT46 axial strains vs time

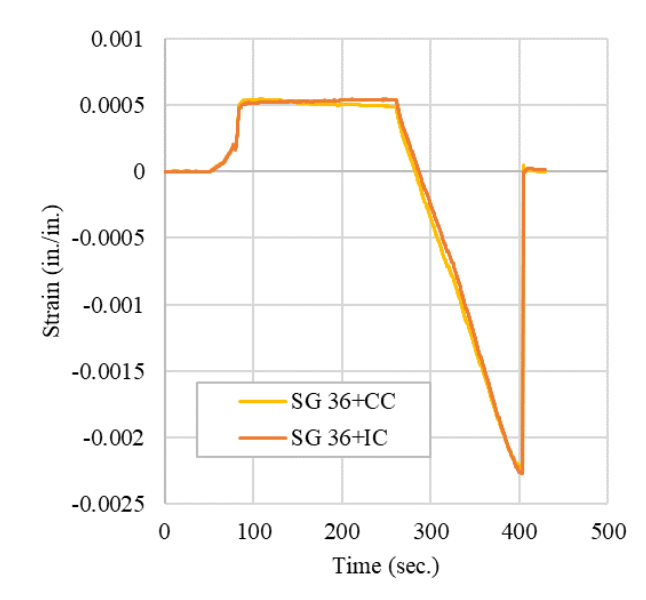


Figure 3.21. PT46 circumferential strains vs time

College of Engineering and Applied Science 428 UCB Boulder, Colorado 80309-0428 Center for Infrastructure, Energy, & Space Testing

t: 303.492.8221

CIEST@colorado.edu website: www.colorado.edu/center/ciest

3.4 Tension Test (PT50)

Figure 3.22 shows the relationship among actuator force, internal pressure, and actuator displacement relative to time for the first PVC pipe tension test produced by Northern Pipe. Displacement was applied at a rate of 1.0 in./min. (25 mm/min.), and the force feedback of the load cell was recorded. Figure 3.23 shows that the maximum force recorded in the load cell was 26.2 kips (116.6 kN) at an actuator displacement of 2.46 in. (62.5 mm). A constant internal water pressure of 65 ± 2 psi (448 \pm 13 kPa) was applied during loading. Figure 3.24 shows the actuator force vs the joint displacement. The joint displacement reached an average of about 1.02 in. (25.9 mm) just before failure. Figure 3.25 shows the bell and spigot connection before the test. A circumferential fracture occurred where the gasket teeth penetrate on the spigot side of the joint, shown in Figure 3.26.

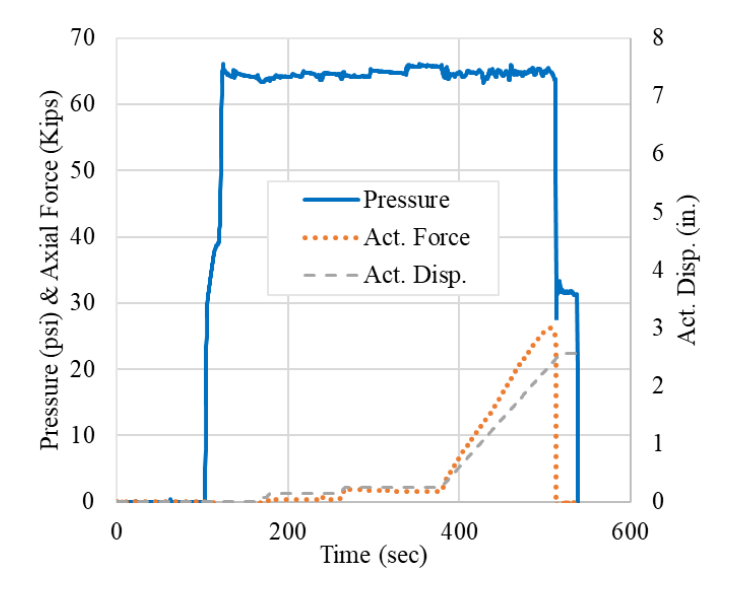


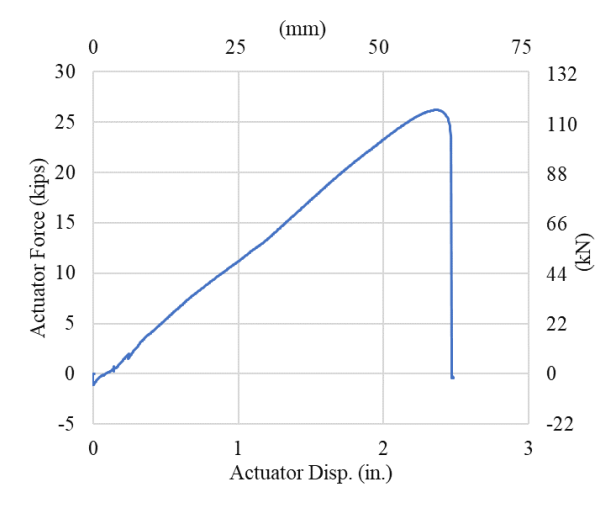
Figure 3.22. Specimen PT50 results for pressure, axial force, and actuator displacement vs time

College of Engineering and Applied Science 428 UCB Boulder, Colorado 80309-0428

t: 303.492.8221 CIEST@colorado.edu

Center for Infrastructure, Energy, & Space Testing

website: www.colorado.edu/center/ciest



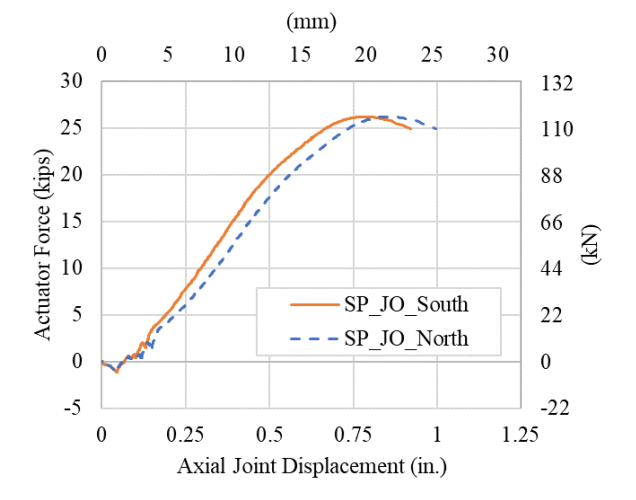


Figure 3.23. PT50 force vs actuator displacement

Figure 3.24. PT50 force vs joint displacements

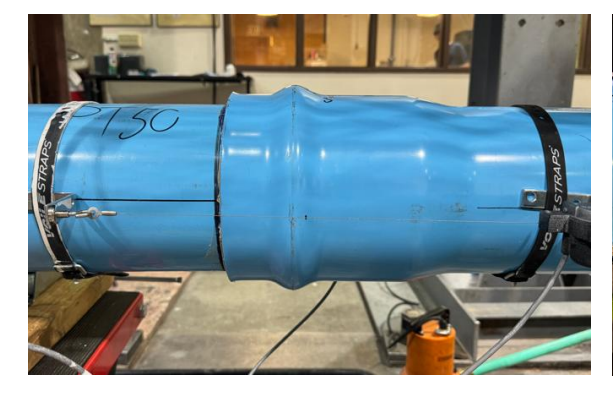




Figure 3.25. East and west side for PT50

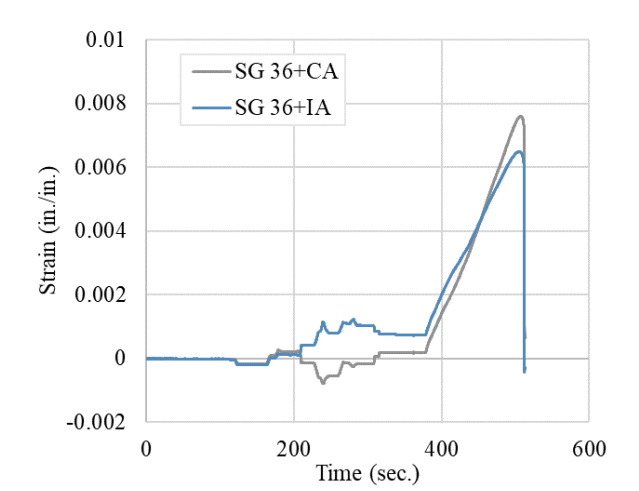
Figure 3.26. Fracture at the spigot for PT50

Figure 3.27 and Figure 3.28 shows the average axial and circumferential strains for the duration of the test. At the start of the test, the system was fully pressurized, and an increase in circumferential strain was observed. Once loading began, the circumferential strains began to decrease, while the axial strains increased. As the actuator applied tensile loading to the system, the pipe began to elongate, causing an increase in axial strains. Due to Poisson's effect, the circumferential strain decreased as the tensile load was applied. The maximum axial strain and circumferential strain were measured at about 0.76% and -0.16% before failure, respectively.

College of Engineering and Applied Science 428 UCB

t: 303.492.8221 CIEST@colorado.edu website:www.colorado.edu/center/ciest

Center for Infrastructure, Energy, & Space Testing Boulder, Colorado 80309-0428



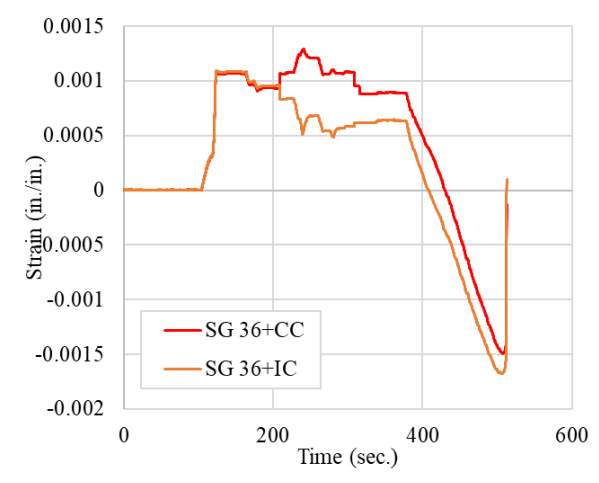


Figure 3.27. PT50 axial strains vs time

Figure 3.28. PT50 circumferential strains vs time

3.5 Tension Test (PT51)

Figure 3.29 also shows the relationship between actuator force, internal pressure, and actuator displacement relative to time for second tension test of Northern Pipe. Displacement was applied at a rate of 1.0 in./min. (25 mm/min.), and the force feedback of the load cell was recorded during the test. A constant internal water pressure of 65 ± 2 psi (448 ± 13 kPa). When the specimen lost its force capacity (t=390 sec), the pressure dropped to about 35 psi and then the joint kept the pressure approximately 20 seconds after that the pressure dropped to 0 (t=410 sec). Figure 3.30 shows that the maximum force recorded in the load cell was 25.7 kips (114.4 kN) at an actuator displacement of 2.31 in. (58.7 mm). Figure 3.31 shows the actuator force vs joint displacement. The joint displacement reached an average of about 0.81 in. (20.6 mm) just before failure. Figure 3.32 shows failure moment at the joint. Failure occurred on the west side (Spigot) of the joint. A circumferential fracture was observed between the end of the spigot and where gasket teeth penetrate on the spigot, as shown in Figure 3.33.

College of Engineering and Applied Science 428 UCB Boulder, Colorado 80309-0428

t: 303.492.8221 CIEST@colorado.edu website:www.colorado.edu/center/ciest

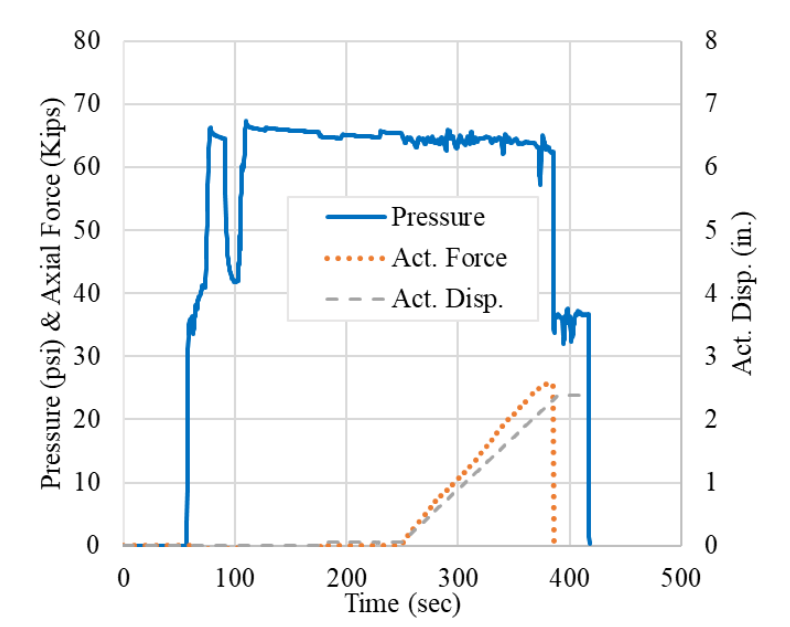


Figure 3.29. Specimen PT51 results for pressure, axial force, and actuator displacement vs time

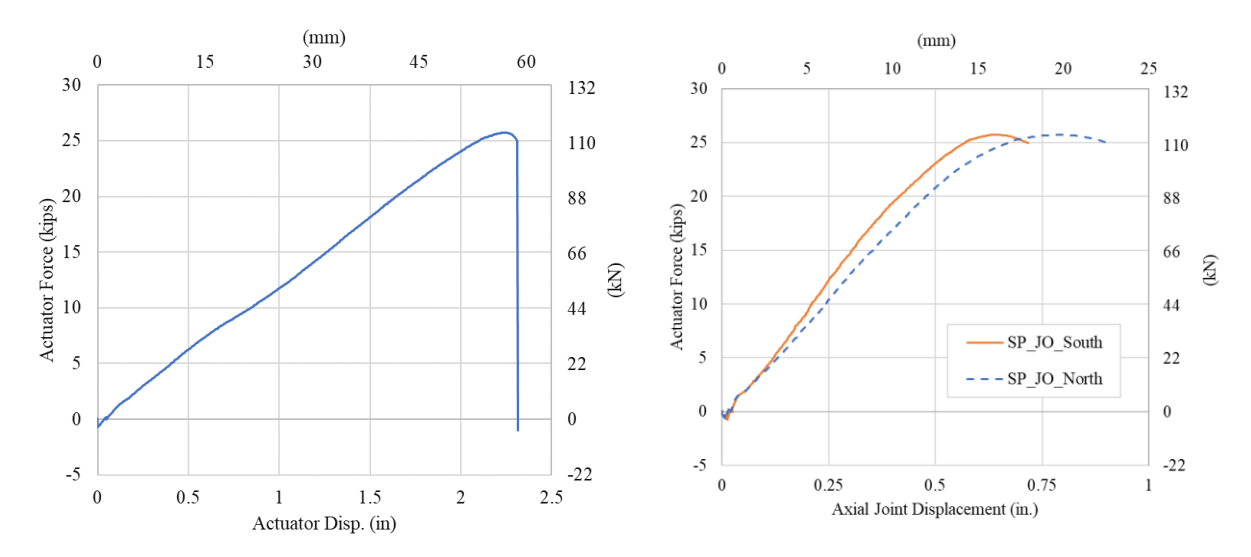


Figure 3.30. PT51 force vs actuator displacement

Figure 3.31. PT51 force vs joint displacements

College of Engineering and Applied Science 428 UCB Center for Infrastructure, Energy, & Space Testing

t: 303.492.8221 CIEST@colorado.edu

Boulder, Colorado 80309-0428 website: www.colorado.edu/center/ciest

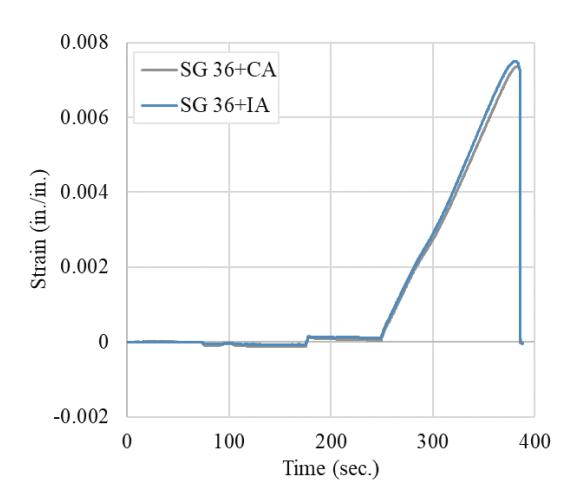




Figure 3.32. Failure moment at joint for PT51

Figure 3.33. Fracture at the spigot for PT51

Figure 3.34 and Figure 3.35 shows the average axial and circumferential strains for the duration of the test. At the start of the test, the system was fully pressurized, and an increase in circumferential strain was observed. Once loading began, the circumferential strains began to decrease, while the axial strains increased. As the actuator applied tensile loading to the system, the pipe began to elongate, causing an increase in axial strains. Due to Poisson's effect, the circumferential strain decreased as the tensile load was applied. The maximum axial strain and circumferential strain were measured at about 0.75% and -0.18% before failure, respectively.



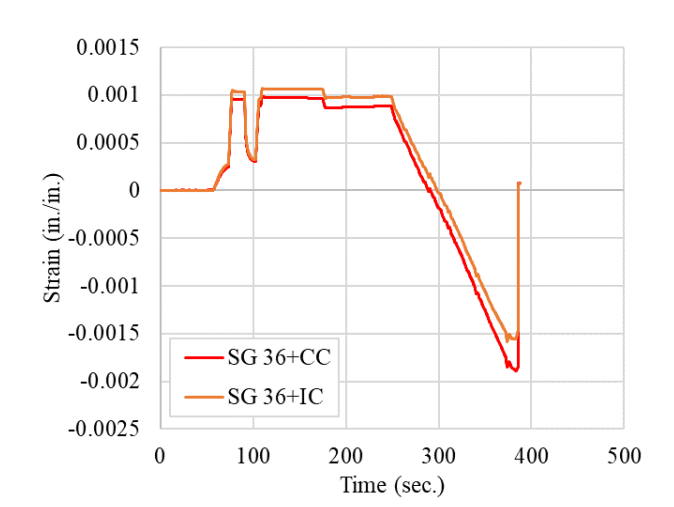


Figure 3.34. PT51 axial strains vs time

Figure 3.35. PT51 circumferential strains vs time

3.6 Tension Test (PT52)

The last tension test performed on PVC pipe manufactured by Northern Pipe was PT52. Figure 3.36 shows the relationship among actuator force, internal pressure, and actuator displacement relative to time. Displacement was applied at a rate of 1.0 in./min. (25 mm/min.), and the force feedback of the load cell College of Engineering and Applied Science 428 UCB Boulder, Colorado 80309-0428 t: 303.492.8221 CIEST@colorado.edu website:www.colorado.edu/center/ciest

Center for Infrastructure, Energy, & Space Testing

was recorded. A constant internal water pressure of 65 ± 2 psi $(448 \pm 13 \text{ kPa})$ was applied during the test. Figure 3.37 also shows that the maximum force recorded in the load cell was 25.2 kips (111.9 kN) at an actuator displacement of 2.20 in. (55.9 mm). Figure 3.38 shows the actuator force vs the joint displacement. The joint displacement reached an average of about 0.7 in. (17.8 mm) at the max force and reached a total of about 0.92 in (23.4 mm) just before failure (22.47 kips). Figure 3.39 shows the bell and spigot connection before the test for PT52. Damage occurred on the gasket, and gasket teeth slipped, as shown in Figure 3.40. Figure 3.41 shows the damage of the RieberLok gasket teeth after the test.

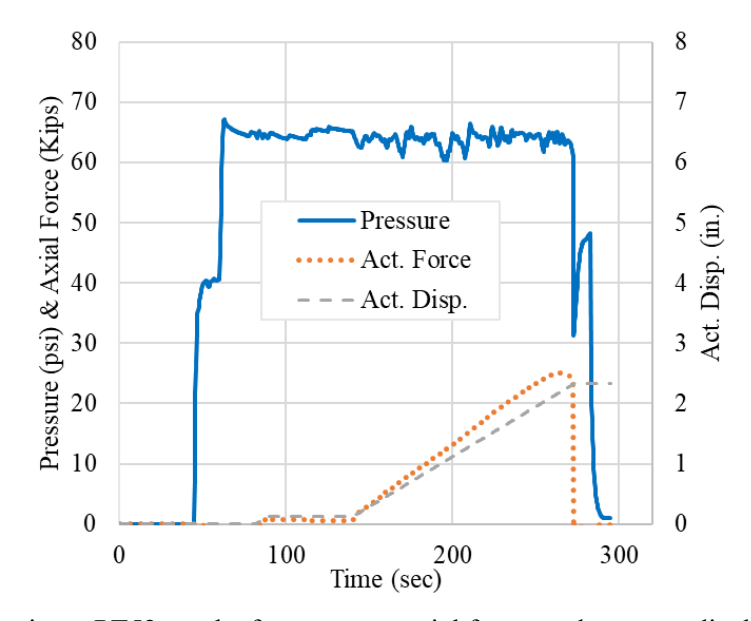
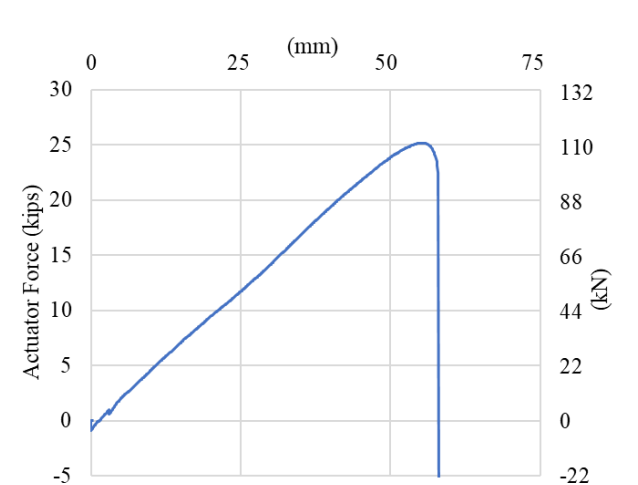
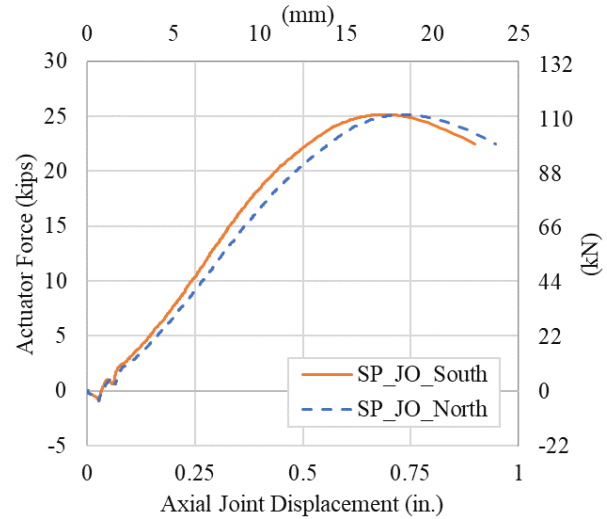


Figure 3.36. Specimen PT52 results for pressure, axial force, and actuator displacement vs time

College of Engineering and Applied Science 428 UCB Boulder, Colorado 80309-0428

t: 303.492.8221 CIEST@colorado.edu website:www.colorado.edu/center/ciest





Actuator Disp. (in.)
Figure 3.37. PT52 force vs actuator displacement

2

3

Figure 3.38. PT52 force vs joint displacements



Figure 3.39. East and west side for PT52



Figure 3.40. After failure for PT52

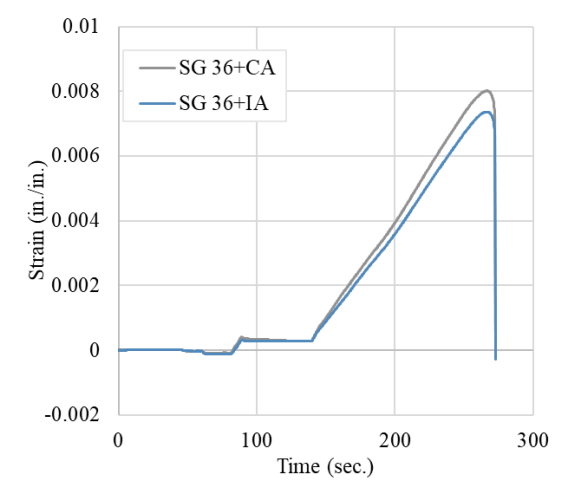


Figure 3.41. After failure for PT52

Figure 3.42 and Figure 3.43 shows the average axial and circumferential strains for the duration of the test. At the start of the test, the system was fully pressurized, and an increase in circumferential strain was observed. Once loading began, the circumferential strains began to decrease, while the axial strains increased. As the actuator applied tensile loading to the system, the pipe began to elongate, causing an increase in axial strains. Due to Poisson's effect, the circumferential strain decreased as the tensile load was applied. The maximum axial strain and circumferential strain were measured at about 0.80% and -0.16% before failure, respectively.

College of Engineering and Applied Science 428 UCB Boulder, Colorado 80309-0428 t: 303.492.8221 CIEST@colorado.edu website:www.colorado.edu/center/ciest

Center for Infrastructure, Energy, & Space Testing



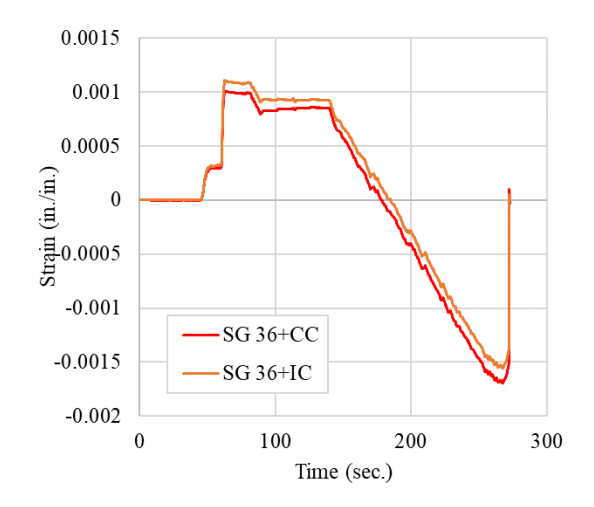


Figure 3.42. PT52 axial strains vs time

Figure 3.43. PT52 circumferential strains vs time

3.7 Tension Test Overview

The following section provides a comparison of the tension tests performed, starting with Table 3.1 which is a summary of the axial test results. Figure 3.44 shows the actuator force relative to the actuator displacement for each tension test. The maximum axial forces under tension test were an average of 26.6 kips (118.3 kN) and 25.7 kips (114.3 kN) for VinylTech and Northern pipes, respectively. The forces and actuator displacements are remarkably consistent for all tension tests. Figure 3.45 shows the joint displacements and axial forces for each test and that the maximum joint displacements ranged between 0.8 in. and 1.02 in. (20.32 and 25.9 mm). Figure 3.46 and Figure 3.47 show the comparison for the axial and circumferential strains, respectively. All tension tests have maximum axial strain values between 0.75% and 0.82%. When we evaluate the performance of the Rieber shape connection, the Northern pipe and VinylTech products have shown remarkably similar force and joint displacement capacity under axial tension tests, however, various failure mechanisms were observed for both types of products. Three distinct failure mechanisms were observed for tension tests: circumferential fracture at the spigot (PT44, PT50, PT51), gasket failure (PT45, PT52), and fracture at either side of the joint (PT46).

College of Engineering and Applied Science 428 UCB

t: 303.492.8221 CIEST@colorado.edu website:www.colorado.edu/center/ciest

Center for Infrastructure, Energy, & Space Testing

Table 3.1. Summary of tension test results (all specimens PVC pipe with RieberLok Gasket)

Boulder, Colorado 80309-0428

Test ID	Pipe	F	Axial orce		Act. sp.	Max A Stra			onnection Disp.
1550 115	Manufacturer	kips	(kN)	in	(mm)	in/in	%	in	(mm)
PT44	VinylTech	26.3	(117)	2.39	(60.7)	0.0082	0.82	0.98	24.9
PT45	VinylTech	25.9	(115)	2.25	(57.2)	0.0078	0.78	0.99	25.1
PT46	VinylTech	27.6	(122)	2.36	(59.9)	0.0081	0.81	0.8	20.3
PT50	Northern	26.2	(116)	2.46	(62.5)	0.0076	0.76	1.02	25.9
PT51	Northern	25.7	(114)	2.31	(58.7)	0.0075	0.75	0.81	20.6
PT52	Northern	25.2	(111)	2.20	(55.9)	0.0080	0.80	0.92	23.4
A	verage	26.15	(115)	2.32	(59.15)	0.0078	0.78	0.92	23.36

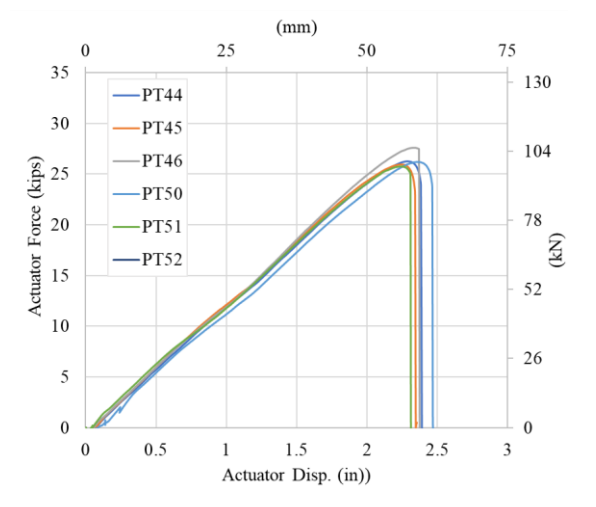


Figure 3.44. Axial force vs actuator displacement for tension tests

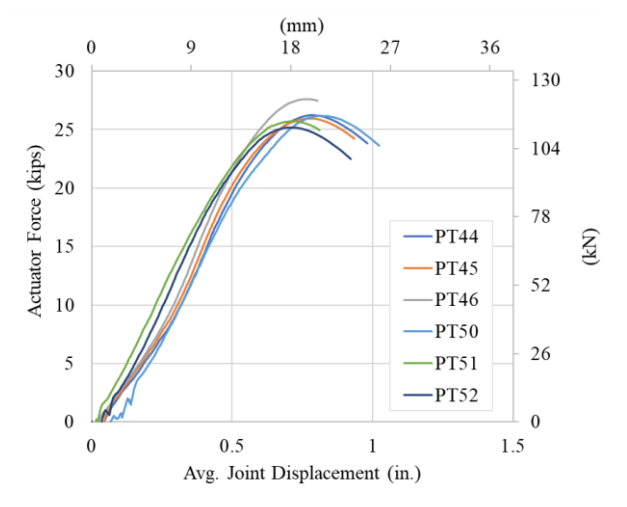


Figure 3.45. Axial force vs average joint displacement for tension tests

Dept. of Civil, Environmental & Architectural Engineering

College of Engineering and Applied Science 428 UCB

t: 303.492.8221 CIEST@colorado.edu

Boulder, Colorado 80309-0428

website: www.colorado.edu/center/ciest

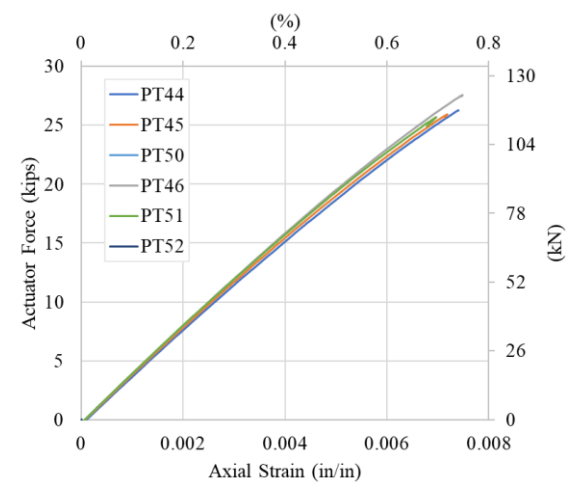


Figure 3.46. Axial force vs axial strain for tension tests

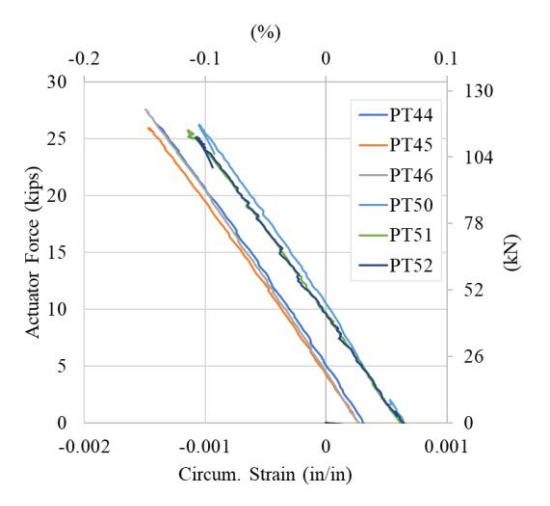


Figure 3.47. Axial force vs circumferential strain for tension tests



College of Engineering and Applied Science 428 UCB

t: 303.492.8221 <u>CIEST@colorado.edu</u> website:<u>www.colorado.edu/center/ciest</u>

4. Axial Cyclic Test Results

The following section presents the results of axial cyclic tests that were performed under varying load protocols. All loading protocols were based on the cyclic loading testing guidance provided by FEMA 464. The cyclic and pull to failure loadings were conducted under displacement control. Every cyclic loading protocol was explained under the related cyclic test. After the cyclic loading sequence, tension loading was conducted to the specimen until failure.

Boulder, Colorado 80309-0428

4.1 Cyclic Test (PS47)

The first cyclic test performed on PVC pipe manufactured by VinylTech was PS47. In this test, loading protocol 1 (LP-1) was conducted under displacement control at a rate of 1 in. per minute for the cyclic sequence (Table 2.1a) and tensile loading. During the cyclic loading, the performed maximum axial displacement in tension and compression cycles is 0.40 in. (10.1 mm). Figure 4.1 shows the water pressure, actuator force, and actuator displacement relative to time during the test. The average water pressure during testing was approximately 73 psi (503 kPa), although changing the internal volume with cyclic loading caused the pressure to fluctuate over the range of approximately 65 – 110 psi (448 – 758 kPa). Generally, when testing pressurized pipe, a pressure regulator is used to keep the pressure constant during fluctuation of the volume of the pipe as displacement is applied. However, during the process of setting up PS47, the regulator was mistakenly not turned on. As seen in Figure 4.1, this resulted in the pressure fluctuating with the volume of the pipe. Figure 4.2 shows the relationship between the actuator force and actuator displacement. The maximum force was 24.5 kips (109.1 kN) and the maximum actuator displacement was 2.08 in. (52.8 mm).

Figure 4.3 shows actuator force vs joint displacement. During cyclic loading, the maximum axial force reached approximately -6.0 kips (26.7 kN) and 5.2 kips (22.9 kN) at the compression part and tension part, respectively. Two string pots were specifically placed on the north and south springlines, precisely 3 inches away from the joint on each side. However, the string pots on the south side malfunctioned during the test, thus only one string pot was used to evaluate joint capacity. After cyclic loading, tensile loading was carried out to failure. There was no leakage observed for PS47 during the loading sequence. The joint displacement measured approximately 0.87 in (22.1 mm) just before failure.

College of Engineering and Applied Science 428 UCB Boulder, Colorado 80309-0428

t: 303.492.8221 <u>CIEST@colorado.edu</u> website:<u>www.colorado.edu/center/ciest</u>

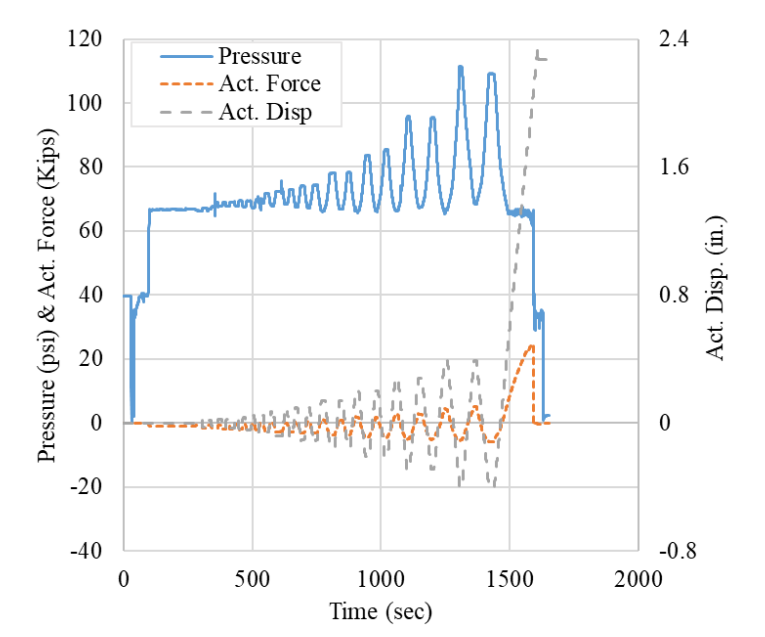
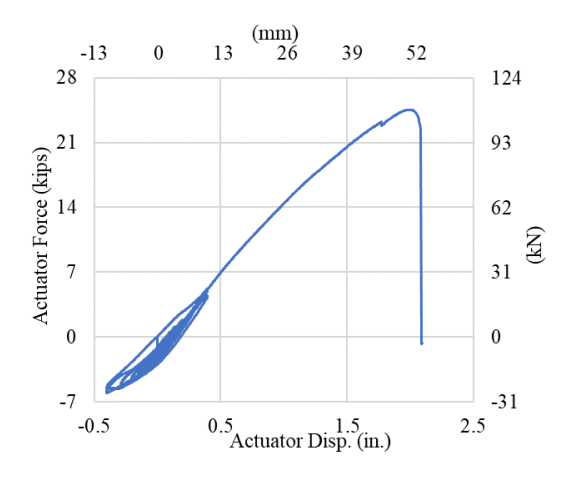


Figure 4.1. PS47 results for internal pressure, actuator displacement and axial force vs. time



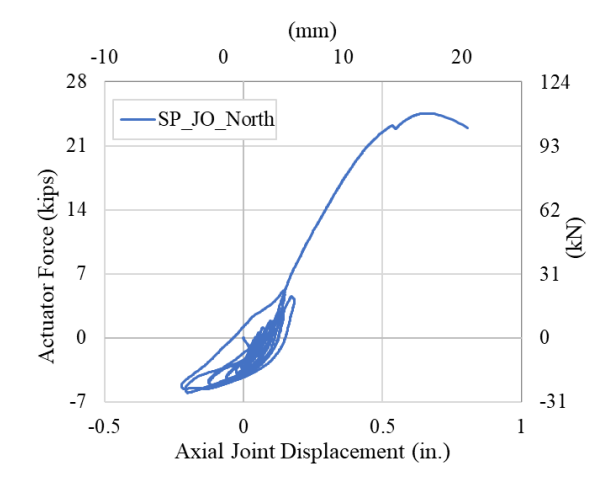


Figure 4.2. PS47 force vs. (a) actuator displacement

Figure 4.3. PS47 force vs. joint displacement.

Figure 4.4 and Figure 4.5 show the axial and average circumferential strains for the duration of the test, respectively. At the start of the test, the system was fully pressurized, and an increase in circumferential strain was observed. The maximum axial strain was 0.71% and the maximum circumferential strain was - 0.20%. Images of the joint before and after the test are shown in Figure 4.6 and Figure 4.7, respectively. There was no damage to either of the joints, but the gasket teeth slipped during the tensile loading, causing the connection to lose its pressure capacity.

Center for Infrastructure, Energy, & Space Testing

College of Engineering and Applied Science

428 UCB Boulder, Colorado 80309-0428 t: 303.492.8221 CIEST@colorado.edu website:www.colorado.edu/center/ciest

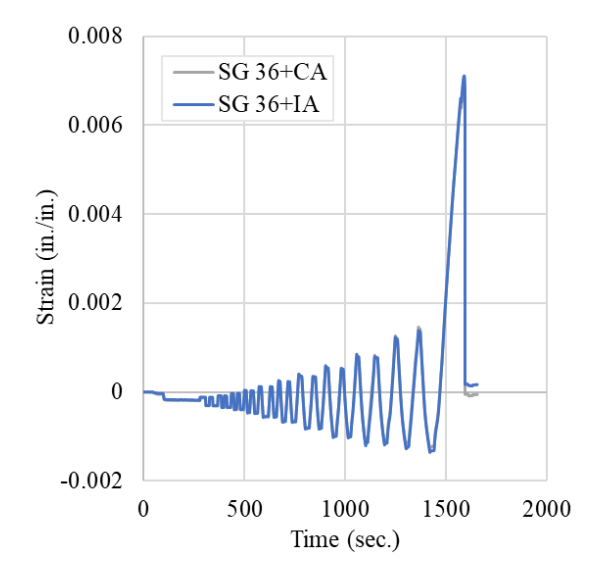


Figure 4.4. PS47 axial strains vs time

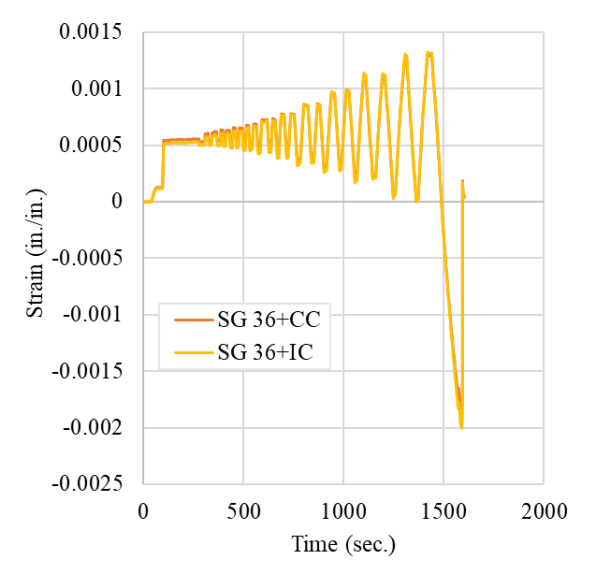


Figure 4.5. PS47 circumferential strains vs time

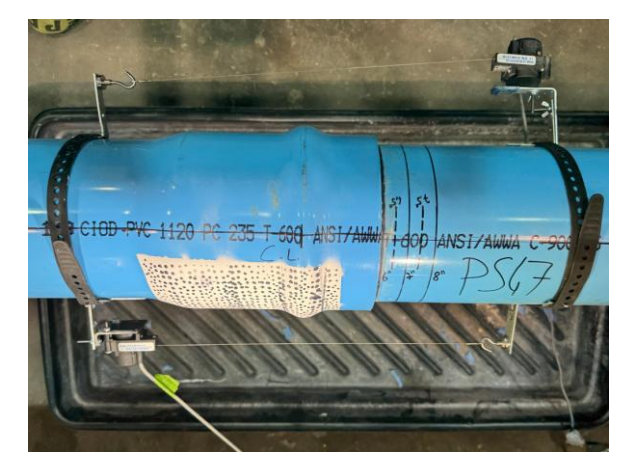


Figure 4.6. PS47 joint before testing



Figure 4.7. PS47 joint failure

4.2 Cyclic Test (PS48)

The second cyclic test performed on PVC pipe manufactured by VinylTech was PS48. In this test, the loading protocol 2 (LP-2) was used under displacement control at a rate of 1 in. per minute for the cyclic sequence (Table 2.1b). During the cyclic loading, the conducted maximum axial displacement in tension and compression cycles is 0.83 in. (21.2 mm). Figure 4.8 shows the water pressure, actuator force, and actuator displacement relative to time during the test. The average water pressure during testing was

College of Engineering and Applied Science 428 UCB

t: 303.492.8221 CIEST@colorado.edu website:www.colorado.edu/center/ciest

Center for Infrastructure, Energy, & Space Testing

approximately 65 psi (448 kPa). Modifications to the pressure regulating system allowed for more constant internal pressure during cycles than the previous test (PS47).

Boulder, Colorado 80309-0428

Figure 4.9 shows the relationship between the actuator force and actuator displacement. The maximum force was 21.9 kips (97.5 kN), and the maximum actuator displacement was 1.6 in. (40.6 mm). Figure 4.10 shows actuator force vs joint displacement. During cyclic loading, the maximum axial force reached -5.8 kips (25.8 kN) and 15.04 kips (66.9 kN) in the compressive and tension parts, respectively. After cyclic loading, tensile loading was carried out to failure. The joint displacement measured approximately 0.55 in (13.97 mm) just before failure.

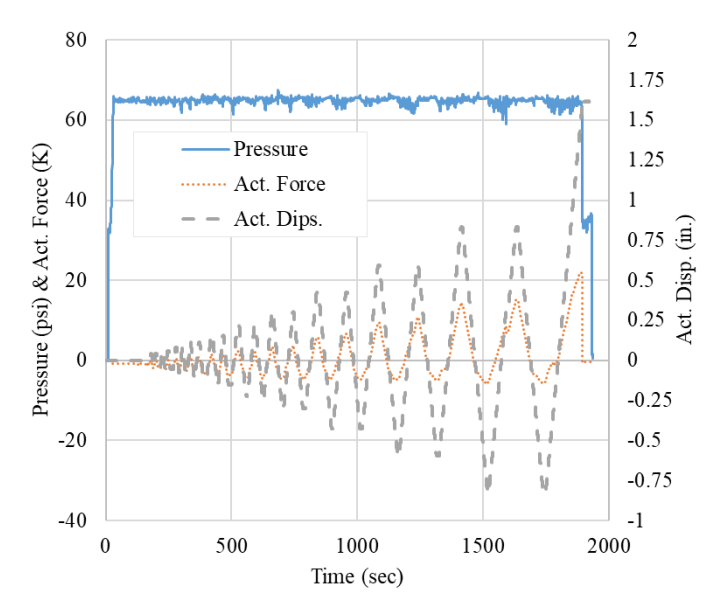
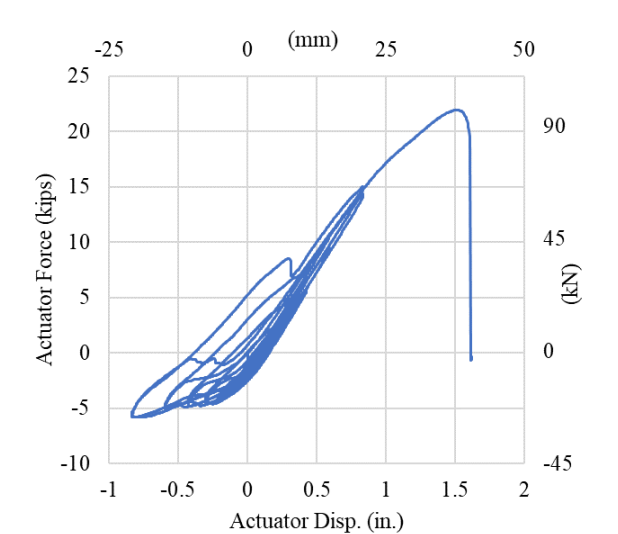


Figure 4.8. PS48 results for internal pressure, actuator displacement and axial force vs. time

t: 303.492.8221 CIEST@colorado.edu website:www.colorado.edu/center/ciest

Center for Infrastructure, Energy, & Space Testing



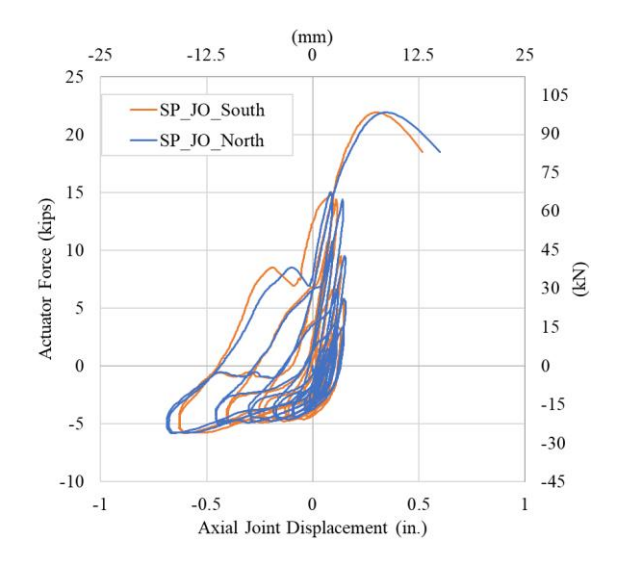


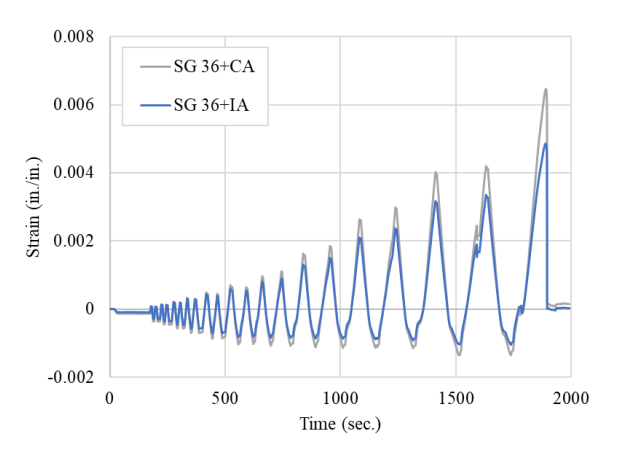
Figure 4.9. PS48 force vs. (a) actuator displacement

Figure 4.10. PS48 force vs. joint displacement.

Figure 4.11 and Figure 4.12 show the axial and average circumferential strains for the duration of the test, respectively. At the start of the test, the system was fully pressurized, and an increase in circumferential strain was observed. The maximum axial strain was 0.64% and the maximum circumferential strain was -0.16% before the failure. Figure 4.13 and Figure 4.14 show the joint before testing and after failure, respectively. The failure was caused by circumferential fracture of the spigot where the RieberLok gasket teeth engage with the pipe. No leakage was observed for PS48 during the cyclic loading sequence.

0.0015

0.001



0.0005

-0.001

-0.0015

-0.002

0 500 1000 1500

Time (sec.)

Figure 4.11. PS48 axial strains vs time

Figure 4.12. PS48 circumferential strains vs time

2000

t: 303.492.8221 CIEST@colorado.edu website:www.colorado.edu/center/ciest

Center for Infrastructure, Energy, & Space Testing

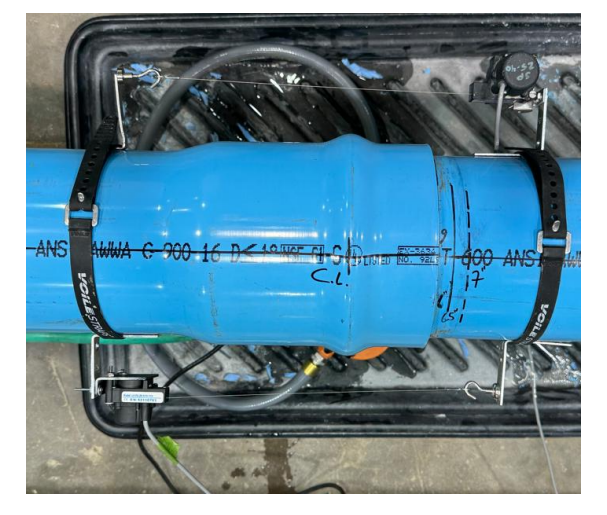


Figure 4.13. PS48 joint before testing



Figure 4.14. PS48 joint fracture at the west side

4.3 Cyclic Test (PS49)

Figure 4.15 shows the water pressure, actuator force, and actuator displacement relative to time for third cyclic test of VinylTech. The loading protocol 2 (LP-2) was used under displacement control at a rate of 1 in. per minute for the cyclic sequence (Table 2.1b) for PS49. The average water pressure during the loading was approximately 65 psi (448 kPa). Figure 4.16 shows the relationship between the actuator force and actuator displacement. The maximum force was 23.0 kips (102.4 kN), and the maximum actuator displacement was 1.71 in. (43.43 mm). Figure 4.17 shows actuator force vs joint displacement. During cyclic loading, the maximum axial force reached -5.9 kips (26.1 kN) and 15.2 kips (67.5 kN) in the compressive and tension parts, respectively. During the cyclic loading process, small leaks were observed in the middle of the compressive loading phase in the 19th and 20th cycles. After the cyclic loading sequence, tensile loading was carried out to failure. The joint displacement measured approximately 0.51 in (12.95 mm) just before failure.

College of Engineering and Applied Science 428 UCB

t: 303.492.8221 <u>CIEST@colorado.edu</u> website:<u>www.colorado.edu/center/ciest</u>

Center for Infrastructure, Energy, & Space Testing

Boulder, Colorado 80309-0428

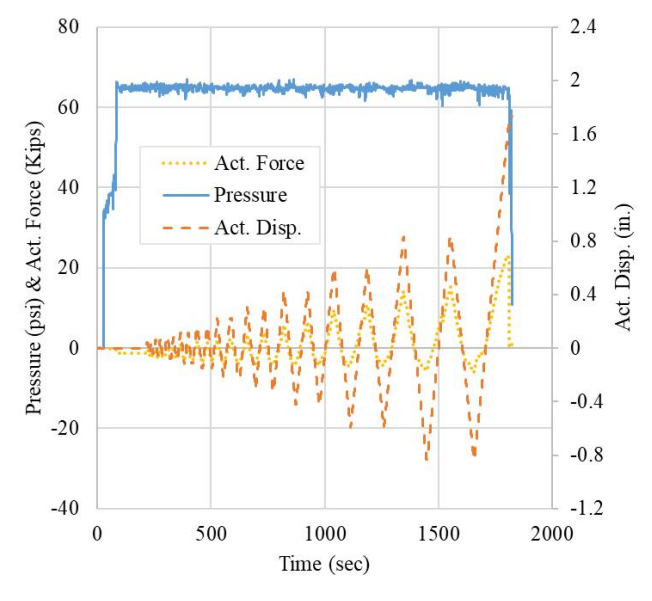


Figure 4.15. PS49 results for internal pressure, actuator displacement and axial force vs. time

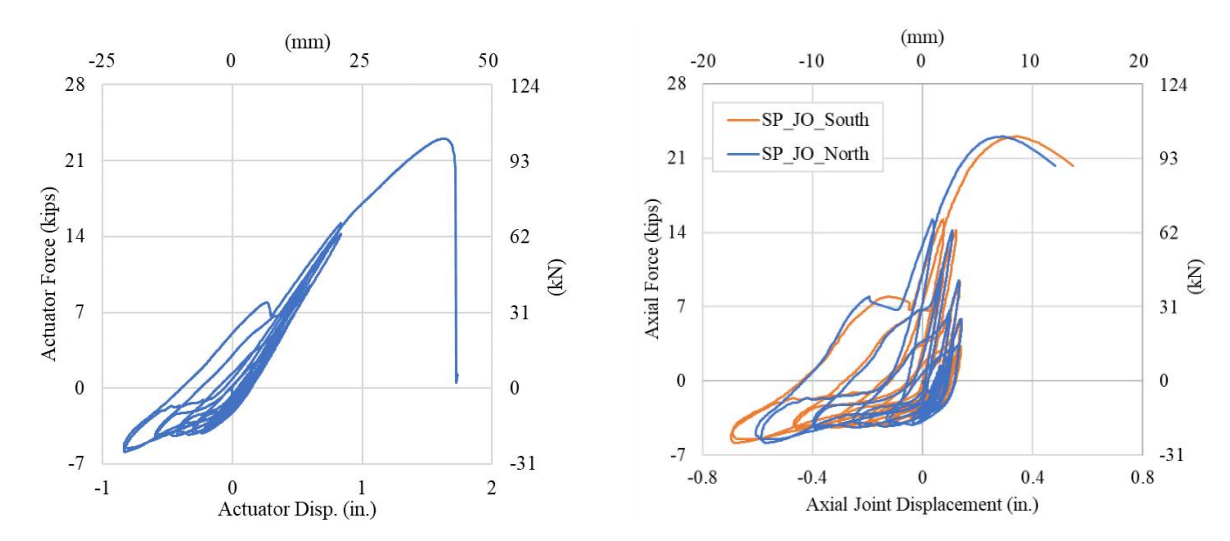


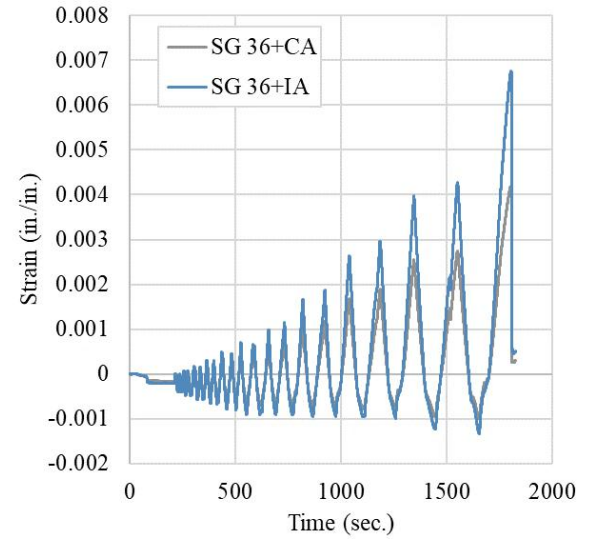
Figure 4.16. PS49 force vs. actuator displacement

Figure 4.17. PS49 force vs. joint displacement

Figure 4.18 and Figure 4.19 show the axial and circumferential strains for the duration of the test, respectively. At the start of the test, the system was fully pressurized, and a decrease in circumferential strain was observed. The maximum axial strain was 0.67% and the maximum circumferential strain was -0.13%. Figure 4.20 and Figure 4.21 show the joint before testing and after failure, respectively. There was no damage to either of the joints, but the gasket teeth slipped during the tensile loading, causing the connection to lose its pressure capacity.

t: 303.492.8221 CIEST@colorado.edu website:www.colorado.edu/center/ciest

Center for Infrastructure, Energy, & Space Testing



0.001 0.0005 0 Strain (in./in.) -0.0005 SG 36+CC -0.001 SG 36+IC -0.0015 -0.002 0 500 1000 1500 2000 Time (sec.)

Figure 4.18. PS49 axial strains vs time

Figure 4.19. PS49 circumferential strains vs time





Figure 4.20. PS49 joint before testing

Figure 4.21. PS49 joint failure

4.4 Cyclic Test (PS53)

The first cyclic test performed on PVC pipe manufactured by Northern Pipe was PS53. The loading protocol 2 (LP-2) was used under displacement control at a rate of 1 in. per minute for the cyclic sequence (Table 2.1b) for PS53. Figure 4.22 shows the water pressure, actuator force, and actuator displacement relative to time during the test. At the beginning of the test, a malfunction of the pressure regulator caused the fluctuations up to t=500 sec. The average water pressure during the test was about 65 psi (448 kPa) until the first leakage in the 18th cycle. During the leaks pressure dropped to approximately 55 psi (380 kPa).

t: 303.492.8221 CIEST@colorado.edu website:www.colorado.edu/center/ciest

Center for Infrastructure, Energy, & Space Testing

Figure 4.23 shows the relationship between the actuator force and actuator displacement. The maximum force was 23.2 kips (103.3 kN), and the maximum actuator displacement was 1.62 in. (41.14 mm). Figure 4.24 shows actuator force vs joint displacement. During cyclic loading, the max axial force reached -4.5 kips (20.1 kN) and 17.6 kips (78.5 kN) in compressive and tensile loading, respectively. During the cyclic loading process, a steady leak was first observed at the onset of the tension loading phase in the 18th cycle and continued throughout this phase. As the loading transitioned into the compressive phase in the 19th cycle, the leak persisted and extended through the entire compressive phase and into the subsequent tension phase of the same cycle. This pattern of steady leakage continued into the 20th cycle and extended into the start of the pull-to-failure loading. The leakage finally ceased when the gasket teeth engaged the pipe again (t=2000 sec). The tensile loading was carried out to failure. The joint displacement measured averaged 0.30 in (7.62 mm) just before failure.

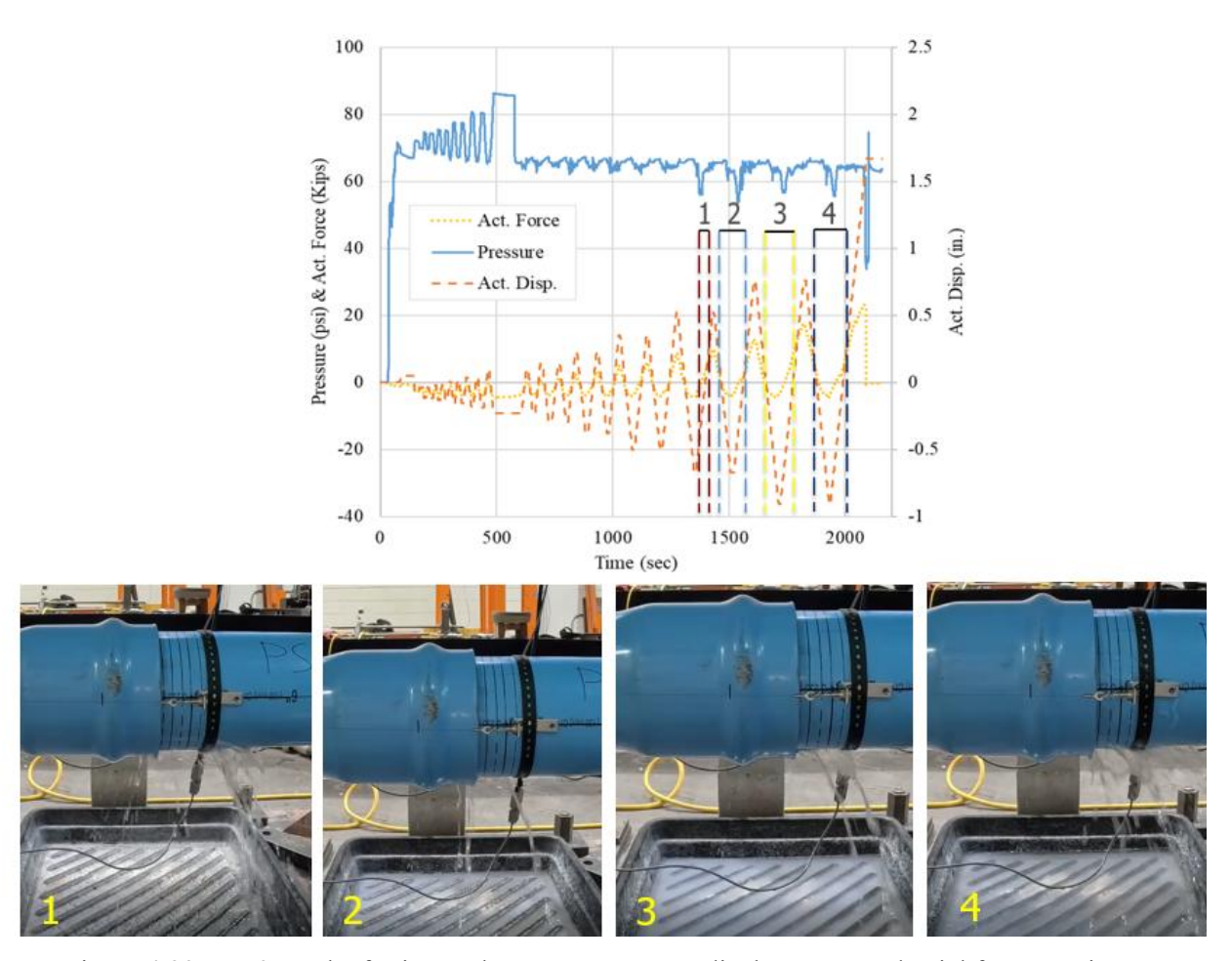
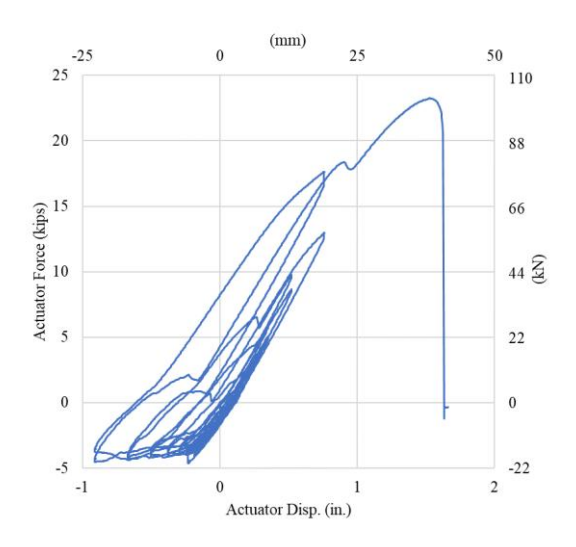


Figure 4.22. PS53 results for internal pressure, actuator displacement and axial force vs. time

t: 303.492.8221 <u>CIEST@colorado.edu</u> website:<u>www.colorado.edu/center/ciest</u>

Center for Infrastructure, Energy, & Space Testing

Figure 4.25 and Figure 4.26 show the axial and average circumferential strains for the duration of the test, respectively. At the start of the test, the system was fully pressurized, and an increase in circumferential strain was observed. The maximum axial strain was 0.67% and the maximum circumferential strain was -0.12%. Figure 4.27 shows the failure moment at the bell side of the joint. During the final compression cycle, joint displacements reached -0.82 in. (20.8 mm). This significant displacement adversely impacted the capacity of the bell side. Consequently, during tensile loading, a circumferential fracture occurred at the bell, as shown in Figure 4.28. This observation is crucial as it highlights the pronounced impact of cyclic loading on the structural integrity and failure mechanisms of the joint.



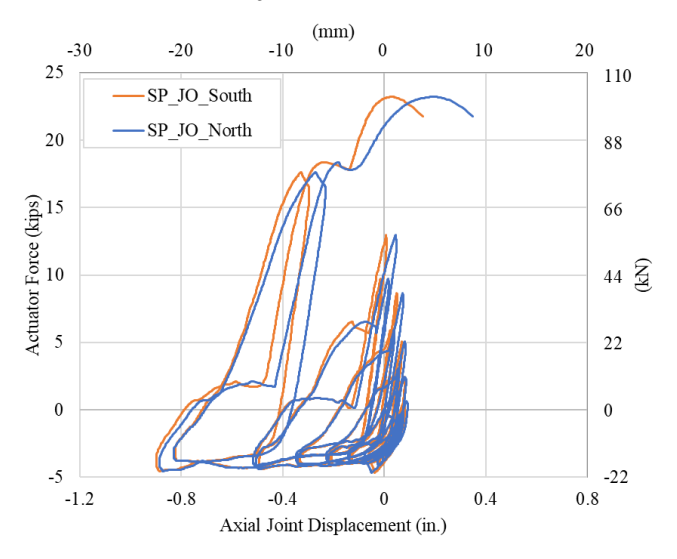


Figure 4.23. PS53 force vs. actuator displacement

Figure 4.24. PS53 force vs. joint displacement

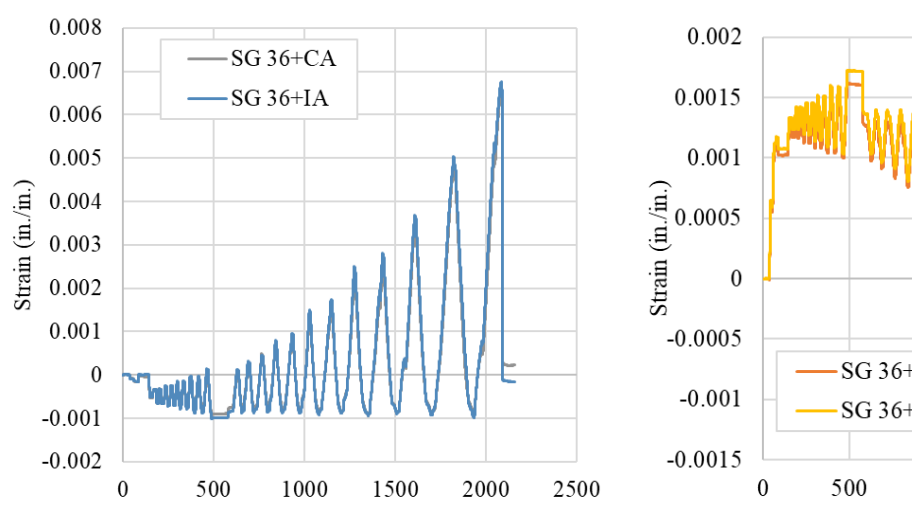
Center for Infrastructure, Energy, & Space Testing

College of Engineering and Applied Science

<u>CIEST@colorado.edu</u> website:<u>www.colorado.edu/center/ciest</u>

t: 303.492.8221

428 UCB Boulder, Colorado 80309-0428



0.002 0.0015 0.0005 -0.0005 -0.0005 -0.0015 0 500 1000 1500 2000 2500 Time (sec.)

Figure 4.25. PS53 axial strains vs time

Time (sec.)

Figure 4.26. PS53 circumferential strains vs time



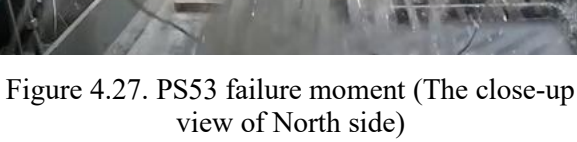




Figure 4.28. PS53 fracture at the bell side of the joint (The close-up view of South side)

4.5 Cyclic Test (PS54)

The second cyclic test performed on PVC pipe manufactured by Northern Pipe was PS54. The loading protocol 2 (LP-2) was used at a rate of 9 in. per minute for the cyclic sequence for PS54. In this test, LP-2 converted the time history loading data. Using the same peak displacement values for the cyclic sequence, a time history of approximately 150 seconds was obtained, as shown in Figure 4.29. After the cyclic sequence, tensile loading was performed under displacement control at a rate of 1 in. per minute. Figure

College of Engineering and Applied Science 428 UCB

Boulder, Colorado 80309-0428

<u>CIEST@colorado.edu</u> website:<u>www.colorado.edu/center/ciest</u>

t: 303.492.8221

Center for Infrastructure, Energy, & Space Testing

4.30 shows the water pressure, actuator force, and actuator displacement relative to time during the test. The average water pressure beginning of the test was approximately 65 psi (448 kPa). With the initiation of the cyclic loading sequence, water pressure fluctuations were observed within the range of 60-70 psi (415 - 483 kPa). At the start of the final two cycles (t=380 sec), steady leaks were detected, causing the pressure to drop to approximately 55 psi (380 kPa). Figure 4.31 and Figure 4.23 shows the relationship between the actuator force and actuator displacement. The maximum force was 21.3 kips (94.6 kN), and the maximum actuator displacement was 1.85 in. (47.0 mm). Figure 4.32 shows actuator force vs joint displacement. During cyclic loading, the max axial force reached -4.6 kips (20.5 kN) and 12.5 kips (55.8 kN) in the compressive and tension parts, respectively. During the cyclic loading process, a steady leak was first observed at the onset of the tension loading phase in the last cycle (20th cycle) and continued throughout this tension phase. At the middle of the compressive phase, a steady leak occurred again and continued to the end of cyclic loading. After cyclic loading, tensile loading was carried out to failure. The joint displacement measured approximately 0.65 in. (16.51 mm) just before failure.

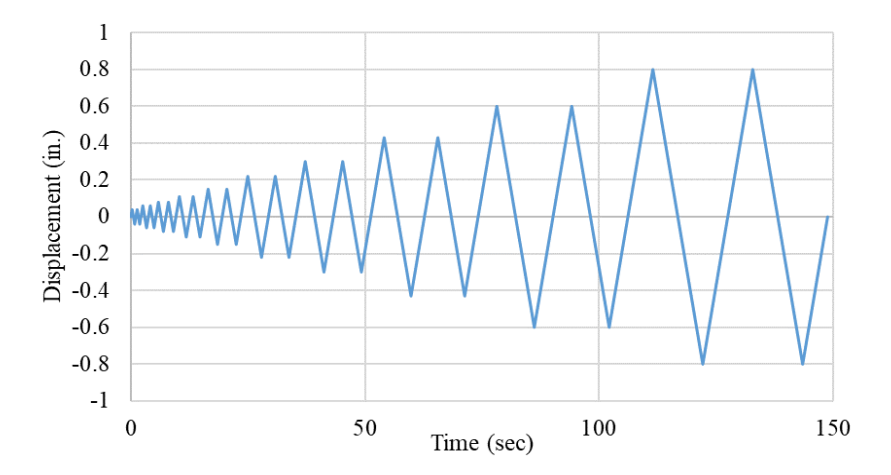


Figure 4.29. The cyclic loading sequence for PS54

t: 303.492.8221 CIEST@colorado.edu website:www.colorado.edu/center/ciest

Center for Infrastructure, Energy, & Space Testing

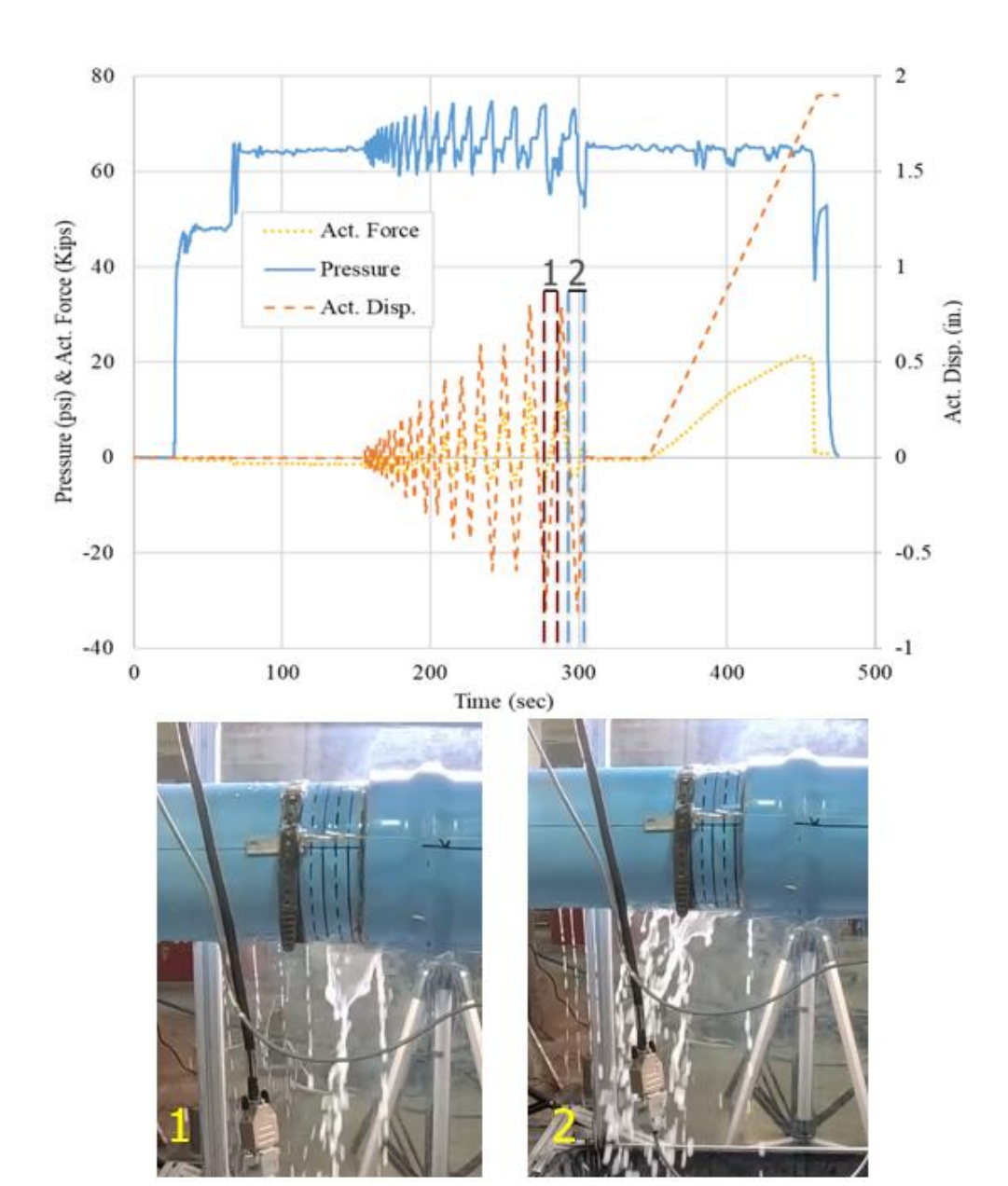
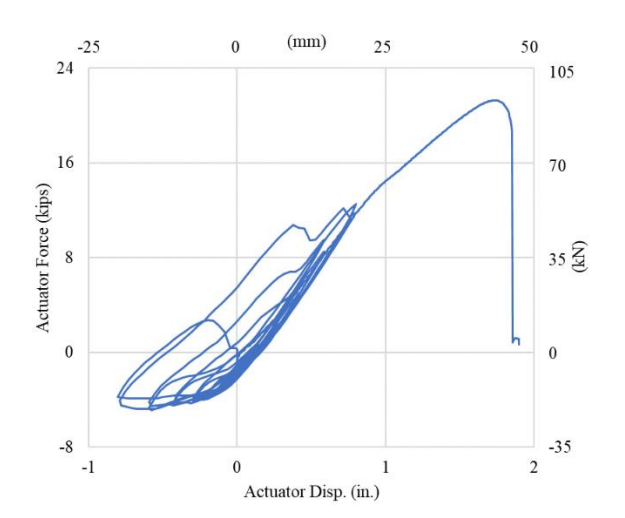


Figure 4.30. PS54 results for internal pressure, actuator displacement and axial force vs. time

t: 303.492.8221 CIEST@colorado.edu website:www.colorado.edu/center/ciest

Center for Infrastructure, Energy, & Space Testing

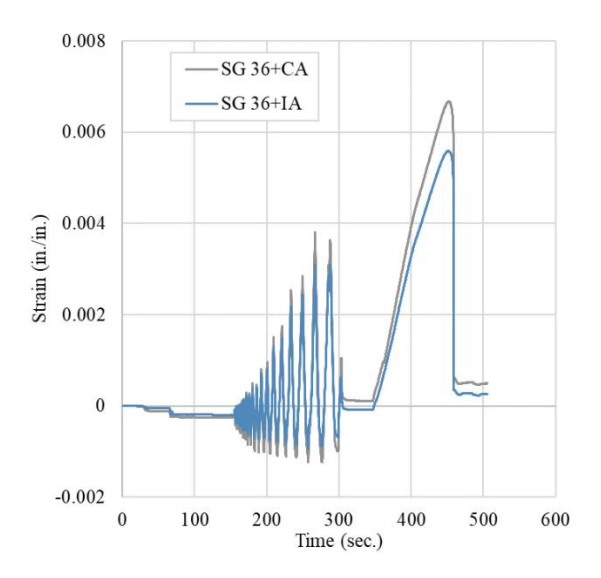


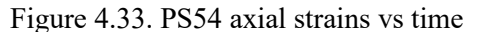
(mm) -20 -15 -10 10 15 20 24 105 SP JO South -SP_JO_North 16 70 Actuator Force (kips) 35 Z -35 0.6 Axial Joint Displacement (in.)

Figure 4.31. PS54 force vs. actuator displacement

Figure 4.32. PS54 force vs. joint displacement

Figure 4.33 and Figure 4.34 show the axial and average circumferential strains for the duration of the test, respectively. At the start of the test, the system was fully pressurized, and an increase in circumferential strain was observed. The maximum axial strain was 0.66% and the maximum circumferential strain was -0.13%. Figure 4.35 and Figure 4.36 show the joint before testing and after failure, respectively. There was no damage to either of the joints, but the gasket teeth slipped during the tensile loading, causing the connection to lose its pressure capacity.





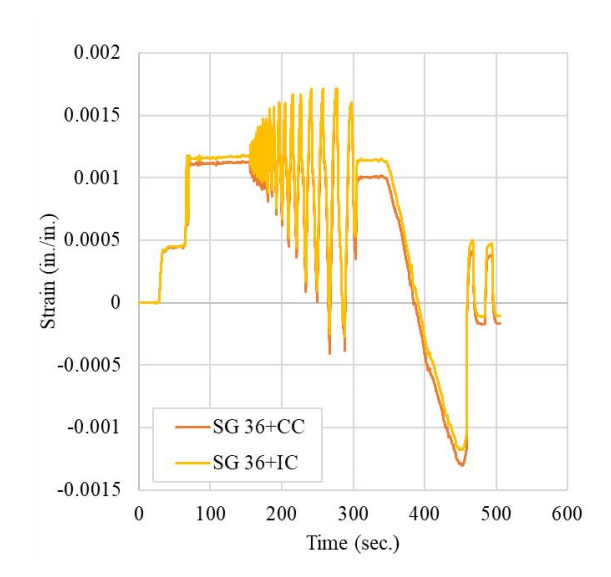


Figure 4.34. PS54 circumferential strains vs time

t: 303.492.8221 CIEST@colorado.edu website:www.colorado.edu/center/ciest

Center for Infrastructure, Energy, & Space Testing





Figure 4.35. PS54 joint before testing

Figure 4.36. PS54 joint failure

4.6 Cyclic Test (PS55)

The last cyclic test performed on PVC pipe manufactured by Northern Pipe was PS55. The loading protocol 2 (LP-2) was used at a rate of 1 in. per minute for the cyclic sequence for PS55. By following the same procedure as the previous cyclic test's loading protocol, LP-2 converted the time history loading data. Using the same peak displacement values for the cyclic sequence, a time history of approximately 22.5 minutes was obtained, as shown in Figure 4.37. After the cyclic loading, tensile loading was performed under displacement control at a rate of 1 in. per minute. Figure 4.38 shows the water pressure, actuator force, and actuator displacement relative to time during the test. The average water pressure until the tension part of the last cycle was approximately 65 psi (448 kPa). The water pressure dropped to 55 psi (380 kPa) during the last cycle loading. During the cyclic loading process, a steady leak was first observed at the onset of the tension loading phase in the last cycle (20th cycle) and continued throughout this tension phase. At the middle of the compressive phase, a steady leak occurred again and continued to the end of cyclic loading. After cyclic loading, tensile loading was carried out to failure. Figure 4.39 shows the relationship between the actuator force and actuator displacement. The maximum force was 22.7 kips (100.8 kN), and the maximum actuator displacement was 1.93 in. (49.02 mm). Figure 4.40 shows actuator force vs joint displacement. During cyclic loading, the max axial force reached -3.7 kips (16.5 kN) and 12.9 kips (57.5 kN) in the compressive and tension parts, respectively. The joint displacement measured approximately 0.63 in (16 mm) just before failure.

t: 303.492.8221 CIEST@colorado.edu website:www.colorado.edu/center/ciest

Center for Infrastructure, Energy, & Space Testing

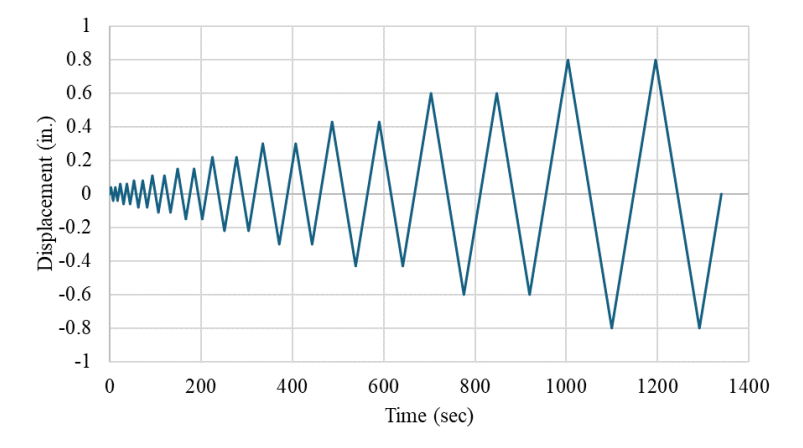


Figure 4.37. The cyclic loading sequence for PS55

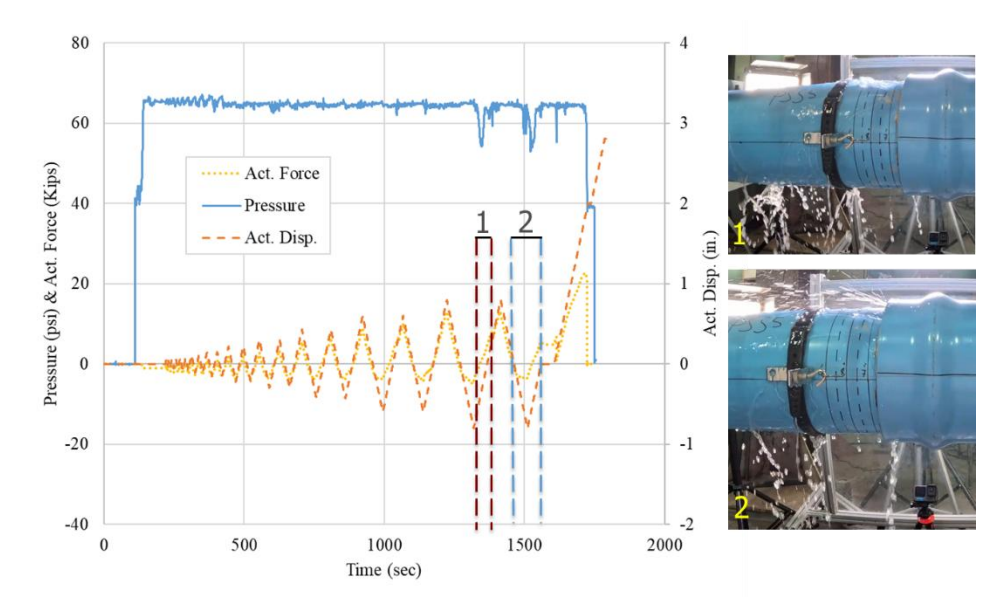
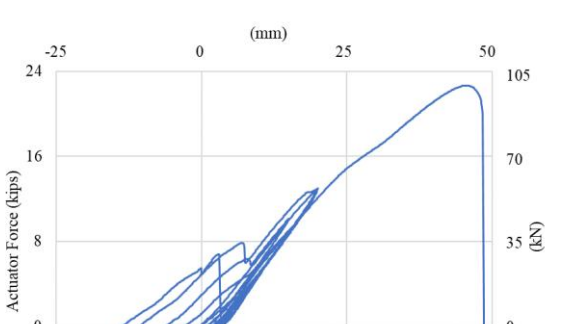


Figure 4.38. PS55 results for internal pressure, actuator displacement and axial force vs. time

-8

College of Engineering and Applied Science 428 UCB Boulder, Colorado 80309-0428 t: 303.492.8221 CIEST@colorado.edu website:www.colorado.edu/center/ciest

Center for Infrastructure, Energy, & Space Testing



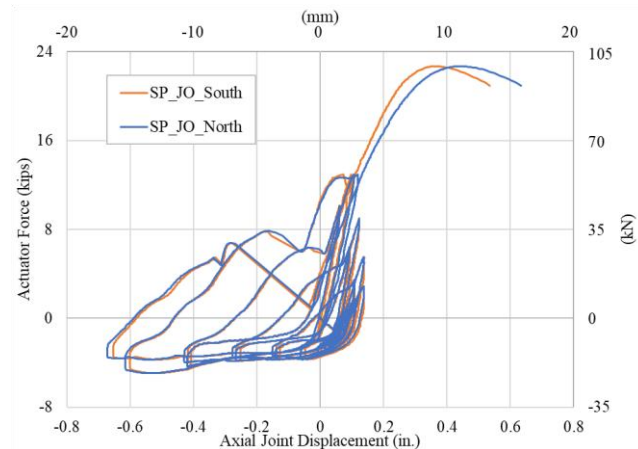


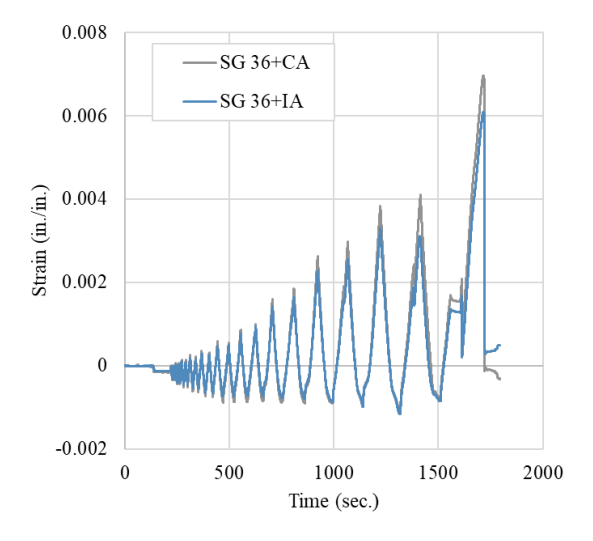
Figure 4.39. PS55 force vs. actuator displacement

Actuator Disp. (in.)

Figure 4.40. PS55 force vs. joint displacement

Figure 4.41 and Figure 4.42 show the axial and average circumferential strains for the duration of the test, respectively. At the start of the test, the system was fully pressurized, and an increase in circumferential strain was observed. The maximum axial strain was 0.69% and the maximum circumferential strain was -0.15%. Figure 4.43 and Figure 4.44 show the joint before testing and after failure, respectively. The failure was caused by circumferential fracture of the spigot where the RieberLok gasket teeth engage with the pipe.

-35



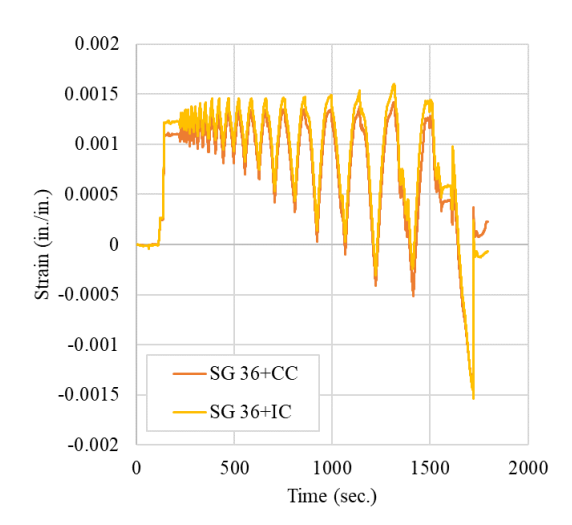


Figure 4.41. PS55 axial strains vs time

Figure 4.42. PS55 circumferential strains vs time

College of Engineering and Applied Science

Center for Infrastructure, Energy, & Space Testing

428 UCB

Boulder, Colorado 80309-0428

t: 303.492.8221 CIEST@colorado.edu

website:www.colorado.edu/center/ciest





Figure 4.43. PS55 joint before testing

Figure 4.44. PS55 joint failure due to fracture on the spigot

4.7 Cyclic Test Overview

Within this project, the six cyclic tests were conducted on PVC pipes manufactured by VinylTech and Northern pipe. The following section provides a comparison of the cyclic tests performed, starting with Table 4.1 which a is a summary of the axial cyclic test results. By using two different loading sequences (LP-1 and LP-2), the axial cyclic tests were performed. The cyclic sequence were performed under displacement control at a rate of 1 in. per minute for all cyclic tests, while the cyclic sequence was conducted at a rate of 9 in. per minute only for PS54. The axial cyclic performance of bell-and-spigot joint capacity was investigated for cyclic loading and tensile loading. Figure 4.45 shows the actuator force relative to the actuator displacement for each cyclic test. The maximum axial forces under cyclic test were an average of 24.5 kips (116 kN) and 23.2 kips (103 kN) for VinylTech and Northern pipes, respectively. The forces and actuator displacements were remarkably similar for all cyclic tests. Figure 4.46 and Figure 4.47 show the joint displacements and axial forces for VinylTech and Northern Pipe, respectively. The maximum joint displacements ranged between 0.3 in. and 0.87 in. (7.6 and 22.1 mm).

Figure 4.48 shows the comparison for the axial strains. All cyclic tests have maximum axial strain values between 0.64% and 0.71%. When we evaluate the performance of the Rieber shape connection, the Northern pipe and VinylTech products have shown remarkably similar force and joint displacement capacity under axial cyclic tests, however, various failure mechanisms were observed for both types of products. Three distinct failure mechanisms were observed for cyclic tests: circumferential fracture at the spigot (PS48 and PS55), gasket failure (PS47, PS49 PS54), and fracture at the bell side of the joint (PS53).

College of Engineering and Applied Science 428 ŬCB

t: 303.492.8221 CIEST@colorado.edu

Center for Infrastructure, Energy, & Space Testing

Boulder, Colorado 80309-0428 website:www.colorado.edu/center/ciest

Table 4.1. Summary of cyclic test results (all specimens PVC pipe with RieberLok Gasket)

Test	Pipe	Loading Protocol	10100		Max Act. Disp.		Max Axial Strain		Joint/connecti on Disp.	
ID	Manufacturer		kips	(kN)	in	(mm)	in/in	%	in	(mm)
PS47	VinylTech	LP-1	24.5	(109)	2.08	(52.83)	0.0071	0.71	0.87	(22.09)
PS48	VinylTech	LP-2	21.9	(97)	1.6	(40.64)	0.0064	0.64	0.55	(13.97)
PS49	VinylTech	LP-2	23.0	(102)	1.71	(43.43)	0.0067	0.67	0.51	(12.95)
PS53	Northern	LP-2	23.2	(103)	1.62	(41.14)	0.0067	0.67	0.30	(7.62)
PS54	Northern	LP-2	21.3	(94)	1.85	(46.99)	0.0066	0.66	0.65	(16.51)
PS55	Northern	LP-2	22.7	(100)	1.93	(49.02)	0.0069	0.69	0.63	(16.00)
Average			22.8	(100)	1.79	(45.67)	0.0067	0.67	0.59	(14.86)

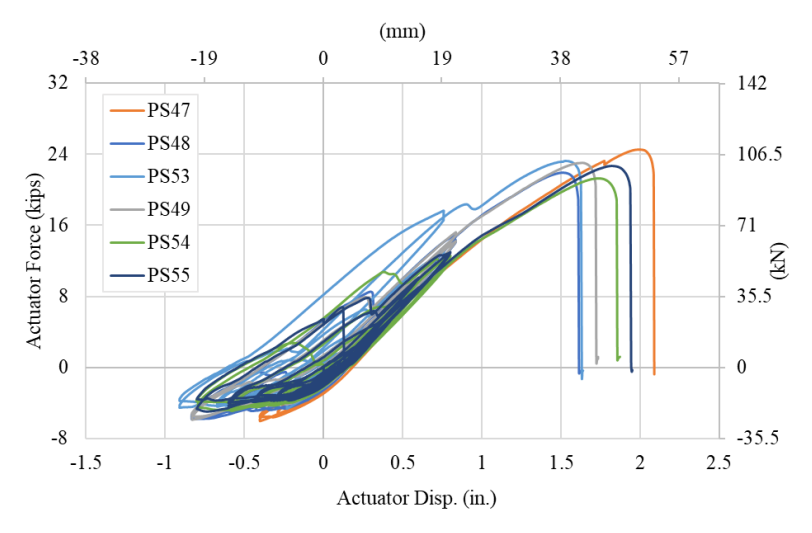


Figure 4.45. Cyclic comparison - force vs. actuator displacement

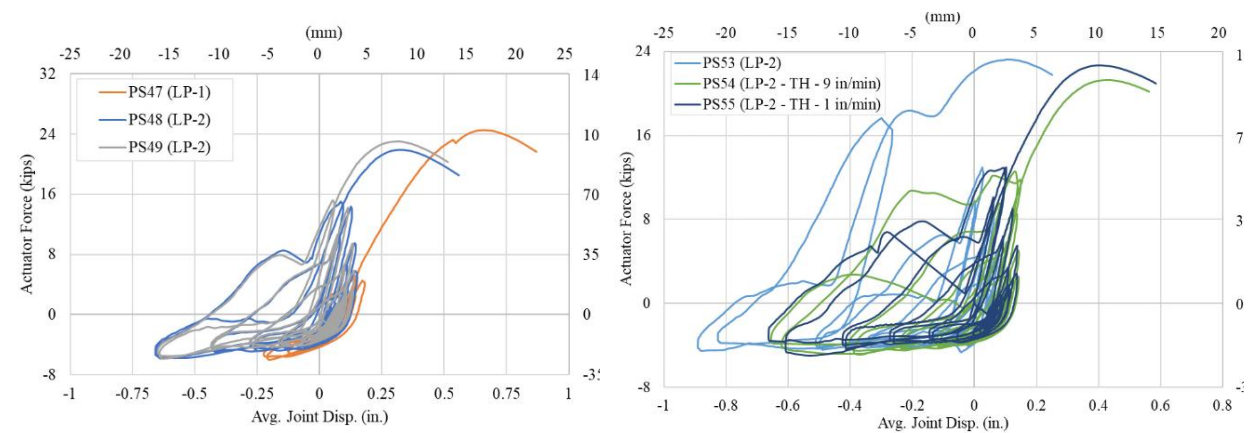


Figure 4.46. Cyclic comparison - force vs. average joint displacement

Figure 4.47. Cyclic comparison - force vs. joint displacement

t: 303.492.8221 CIEST@colorado.edu website:www.colorado.edu/center/ciest

Center for Infrastructure, Energy, & Space Testing

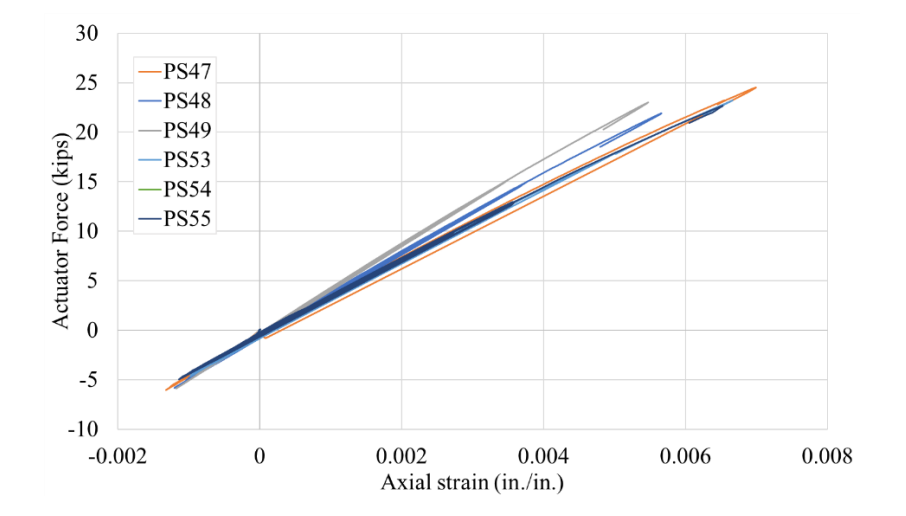


Figure 4.48. Cyclic comparison - force vs. axial strain

5. Conclusions

The tests performed reflect the performance of nominal 6-in. (150-mm) diameter C900 PVC pipe with Riber shape connection. In total, six (6) axial tension tests and six (6) axial cyclic tests were performed on PVC pipes manufactured by VinylTech and Northern Pipe. The work was undertaken in the Center for Infrastructure, Energy, and Space Testing (CIEST) which is affiliated with the Civil, Architectural, and Environmental Engineering Department at the University of Colorado Boulder.

All tests were designed to focus on the evaluation of the axial performance PVC pipe joint with RieberLok gasket under tensile and cyclic loading. The test specimens were subjected to external and internal loading conditions to evaluate the axial performance of pipe joints under significant deformations, such as those caused by earthquake-induced ground deformation, including landsliding, fault rupture, and liquefaction-induced lateral spreading. Upon review of the tension test results, it was observed that three different failure mechanisms were present. Despite various failure mechanisms, the force and joint displacement capacity of the connections were notably consistent across all tension tests, with the average force capacity of the RieberLok shape connection observed at 26.1 kips (116 kN) for all tension tests. In the cyclic tests, no leaks were observed up to 0.4 in. (10.2 mm) of joint displacement during the cyclic loading for VinylTech and Northern Pipe. In addition, although different loading protocols and loading rates were used, the joint force and displacement capacities were remarkably similar for all cyclic tests. The axial force and joint displacement averaged 22.8 kips (101 kN) and 0.59 in. (15 mm), respectively. Notably, cyclical loading slightly reduced the maximum force capacity by about 12.5% when compared to tension only tests. Though



Center for Infrastructure, Energy, & Space Testing

Dept. of Civil, Environmental & Architectural Engineering

College of Engineering and Applied Science 428 UCB

CIEST@colorado.edu website: www.colorado.edu/center/ciest

t: 303.492.8221

some leaks were observed during a few of the cyclic tests, there was no observable impact on the force capacity or joint displacements of the pipe joints for VinylTech and Northern Pipes.

Boulder, Colorado 80309-0428

Acknowledgments

The authors wish to recognize the excellent effort of University of Colorado students and staff that made these experiments successful. Namely, the contributions of graduate students Jessica Ramos and Sina Senji, and undergraduates Simon Abrahamse, Sawer Kuvin, Jonah Cooke, and Ben Hewitt are gratefully acknowledged. Great thanks are extended to CIEST staff members Davis Holt, Kent Polkinghorne, and John Hindman for their constant support and expertise.

References

- Applied Technology Council (ATC). (2007). FEMA 461: Interim Testing Protocols for Determining the Seismic Performance Characteristics of Structural and Nonstructural Components. Redwood, CA: FEMA.
- Ihnotic, C.R. (2019). Seismic Evaluation of Hazard-Resistant Lifelines: Thermoplastic Pipes and Connections. M.Sc. Thesis Report, University of Colorado Boulder, Boulder, CO.
- Wham, B.P., Berger, B.A., Pariya-Ekkasut, C., O'Rourke, T.D., Stewart, H.E., Bond, T.K., & Argyrou, C. (2018). "Achieving Resilient Water Networks – Experimental Performance Evaluation". Proceedings: Eleventh U.S. National Conference on Earthquake Engineering (11NCEE) (Vol. 10, p. 11). Los Angeles, CA. Retrieved from http://www.scopus.com/inward/record.url?eid=2-s2.0-85085619371&partnerID=MN8TOARS
- Wham, B.P., Ihnotic, C.R., Balcells, D., & Anderson, D.K. (2019). "Performance Assessment of Pipeline System Seismic Response". Proceedings: JWWA/WRF/CTWWA Water System Seismic Conference. Los Angeles, CA: JWWA/WRF/CTWWA.